

Permanent deformation analysis of asphalt mixtures using soft computing techniques

Mohammad Reza Mirzahosseini^a, Alireza Aghaeifar^b, Amir Hossein Alavi^c, Amir Hossein Gandomi^{c,d}, Reza Seyednour^{e,*}

^a Department of Civil Engineering, Kansas State University, Manhattan, KS, USA

^b School of Railway Engineering, Iran University of Science and Technology, Tehran, Iran

^c School of Civil Engineering, Iran University of Science and Technology, Tehran, Iran

^d College of Civil Engineering, Tafresh University, Tafresh, Iran

^e Department of Research, University of Social Welfare and Rehabilitation Sciences, Tehran, Iran

ARTICLE INFO

Keywords:

Asphalt pavements
Rutting
Multi expression programming
Artificial neural network
Marshall mix design
Formulation

ABSTRACT

This study presents two branches of soft computing techniques, namely multi expression programming (MEP) and multilayer perceptron (MLP) of artificial neural networks for the evaluation of rutting potential of dense asphalt-aggregate mixtures. Constitutive MEP and MLP-based relationships were obtained correlating the flow number of Marshall specimens to the coarse and fine aggregate contents, percentage of bitumen, percentage of voids in mineral aggregate, Marshall stability, and Marshall flow. Different correlations were developed using different combinations of the influencing parameters. The comprehensive experimental database used for the development of the correlations was established upon a series of uniaxial dynamic creep tests conducted in this study. Relative importance values of various predictor variables of the models were calculated to determine the significance of each of the variables to the flow number. A multiple least squares regression (MLSR) analysis was performed to benchmark the MEP and MLP models. For more verification, a subsequent parametric study was also carried out and the trends of the results were confirmed with the experimental study results and those of previous studies. The observed agreement between the predicted and measured flow number values validates the efficiency of the proposed correlations for the assessment of the rutting potential of asphalt mixtures. The MEP-based straightforward formulas are much more practical for the engineering applications compared with the complicated equations provided by MLP.

© 2010 Elsevier Ltd. All rights reserved.

1. Introduction

Permanent deformation is one of the considerable load-associated distress types affecting the performance of asphalt concrete pavements. The repetitive action of traffic loads results in accumulation of permanent deformations in asphalt pavements (Kaloush, 2001). One of the principal causes of pavement rutting is the permanent deformation. Rutting in asphalt pavement develops progressively with increasing numbers of load application. It usually appears as longitudinal depression in the wheel paths accompanied by small upheavals to the side (Pardhan, 1995). Rutting decreases the useful service life of the pavement and, by affecting vehicle handling characteristics, creates serious hazards for highway users (Alavi, Ameri, Gandomi, & Mirzahosseini, 2010; Gandomi, Alavi, Mirzahosseini, & Moqhadas Nejad, 2010; Sousa,

Craus, & Monismith, 1991). It can decrease drainage capacity of pavements resulting in accumulation of water. Rutting also causes a phenomenon called “bleeding” where the asphalt binder rises to the surface resulting in a very smooth pavement. Another effect of rutting is the reduction in thickness of pavement which increases the occurrence of the pavement failure through fatigue cracking (Bahuguna, 2003). These depressions or ruts are of major concern for at least two reasons: (1) if the surface is impervious, the ruts trap water and hydroplaning is a definite threat particularly for passenger cars, and (2) as the ruts develop in depth, steering increasingly becomes difficult, leading to added safety concerns. Previous studies show that rutting can have remarkable impacts on trucks operational cost (Sousa et al., 1991). The above considerations indicate that rutting is the most harmful distress mechanism in asphalt pavements. According to a comprehensive survey, rutting was considered to be the most serious distress mechanisms in pavements, followed by fatigue cracking and then thermal cracking (FHWA, 1998). As a result, it is important to fully characterize the permanent deformation behavior of asphalt mixes

* Corresponding author.

E-mail addresses: ah_alavi@hotmail.com (A.H. Alavi), a.h.gandomi@gmail.com (A.H. Gandomi), reza.seyednour@gmail.com (R. Seyednour).

under repeated loading and identify the problematic mixes before they are placed in roadways (Alavi, Ameri, et al., 2010; Sousa et al., 1991; Zhou, Scullion, & Sun, 2004).

Evaluation of the rutting potential of asphalt mix has been the focus of much research in pavement engineering over the last decades. Majority of the available permanent deformation models are empirical or semi-mechanistic with limited fundamental material characterization. Unsatisfactory correlations with actual field performance are the common result. Some of the empirical models are derived from limited sets of materials and environmental conditions. Thus, they lack robustness and are not transferable to other conditions. The available rutting evaluation procedures are generally categorized into three main groups: (1) mechanistic-empirical modeling approaches, (2) advanced constitutive modeling approaches, and (3) development of a simple performance test to identify the rutting potential of mixtures during design based on measured fundamental engineering properties and response (Alavi, Ameri, et al., 2010; Kim, 2008, Chap. 11).

The mechanistic-empirical procedures for the rutting prediction couple mechanistic computations of pavement stresses and strains with empirical predictions of the consequent rutting. The earliest mechanistic-empirical rutting models explicitly considered only the strains in the subgrade (e.g., Shook, Finn, Witczak, & Monismith, 1982). Chen, Zaman, and Laguros (1994) provided concise summaries of the evolution of early models for predicting the number of cycles to permanent deformation failure as a function of the vertical compressive strain at the top of the subgrade. Timm and Newcomb (2003) adapted a new model of the form of the earliest models for predicting the asphalt rutting. Permanent strain models are a division of the mechanistic-empirical models by which the permanent vertical compressive strain at the mid-thickness of an asphalt sublayer is related to the number of load cycles, temperature, induced stress level, and other parameters. One of the earliest permanent strain models was that implemented in the VESYS program by different researchers (e.g., Kenis, 1977). Permanent to resilient strain ratio models are another class of the mechanistic-empirical models. The rationale for the permanent to resilient strain ratio models is essentially to consolidate some of the influences of temperature and stress level. Both of these parameters influence the resilient elastic and permanent strains. The permanent strains are normalized with the elastic strains to capture most of the temperature and stress effects. The asphalt rutting model implemented in the NCHRP Project 1–37A mechanistic-empirical design methodology (NCHRP, 2004) is based on this concept. The model has its origins in an extensive laboratory study by Leahy (1989) of the repeated load permanent deformation response of several asphalt concrete specimens. Kaloush (2001) further improved the robustness of the rutting model by combining Leahy's original data with very large number of repeated load permanent deformation test results. Among the mechanistic-empirical procedures, regression models are similar to the permanent strain and strain ratio models since they usually have some mechanistic content such as a computed strain or deflection level (Alavi, Ameri, et al., 2010; Kim, 2008). Many other terms are also included to account for mixture characteristics, environmental variables, and other factors. The most well known of the regression approaches are the Highway Development and Management Model-III (HDM-III) rutting performance models (Kannemeyer & Visser, 1995).

The overall accuracy and robustness of the mechanistic-empirical rutting models still rely heavily upon the quantity and quality of the empirical data used for calibrating the empirical distress model component. Fully mechanistic distress prediction overcomes this limitation. This requires much more sophisticated constitutive models for asphalt concrete behavior (Alavi, Ameri, et al., 2010; Kim, 2008). Recently, significant efforts have been made on

material models that capture the viscoelastic, viscoplastic, and damage response components needed to simulate the behavior of asphalt concrete over its full range of temperatures, loading rates, and stress conditions. These models are implemented into three-dimensional nonlinear finite element codes and applied to realistic test and field scenarios. Gibson, Schwartz, Schapery, and Witczak (2003) and Gibson (2006) proposed one approach toward viscoplastic modeling of asphalt concrete in compression in combination with a Schapery-type viscoelastic continuum damage model (Schapery, 1999). Many researchers also applied the Schapery's model to various aspects of the asphalt concrete behavior (e.g., Chehab, Kim, & Witczak, 2004). The limitation of the finite element-based models is that they are sensitive to the individual cases. Also, a prior knowledge about the nature of the relationships between the data is needed to develop these models.

Another important element in the design of the rut-resistant pavements is screening of asphalt mixtures for the rut susceptibility during mix design. The time to tertiary flow failure is thought to be a good indicator of the rutting resistance of a given mixture (Alavi, Ameri, et al., 2010; Kim, 2008). This can be quantified via the flow number as measured in a repeated load permanent deformation test. Dynamic creep test is found to be one of the best methods for assessing the permanent deformation potential of asphalt mixtures (Kaloush & Witczak, 2002). The curve of accumulated strain against number of load cycles is the most important output of the dynamic creep test. Witczak, Kaloush, Pellinen, El-Basyouny, and Von Quintus (2002) defined the flow number as loading cycle number where tertiary deformation starts. The flow number is more analogous to field conditions since loading of pavement is not continuous. It can be used to identify a mixture's resistance to the permanent deformation by measuring the shear deformation that occurs due to haversine loading (Williams, Robinette, Bausano, & Breakah, 2007). The dynamic creep test is a sensitive and costly test. Thus, it is not always possible to conduct the test. Therefore, developing a relationship between the flow numbers obtained from the dynamic creep test and parameters from the Marshall mix design leads to considerable savings in construction cost and time (Alavi, Ameri, et al., 2010; Gandomi et al., 2010).

Several alternative computer-aided data mining approaches have recently been developed. An instance is pattern recognition systems. These systems learn adaptively from experience and extract various discriminators. Artificial neural networks (ANNs) (Haykins, 1999) are one of the most widely used pattern recognition methods. There have been some researches with the specific objective of applying ANNs to the evaluation of the asphalt pavements performance characteristics. Tarefder, White, and Zaman (2005) constructed ANN-based models to determine a mapping associating mix design and testing factors of asphalt concrete samples with their performance in conductance to flow or permeability. Recently, Tapkin, Cevik, and Usar (2009) utilized ANN for the prediction of the accumulated strain values obtained at the end of repeated creep tests for polypropylene (PP) modified asphalt mixtures. Xiao, Amirkhanian, and Hsein Juang (2009) used a multilayer feed-forward ANN to predict the fatigue life of rubberized asphalt concrete mixtures containing reclaimed asphalt pavement. Ceylan, Schwartz, Kim, and Gopalakrishnan (2009) successfully applied ANNs to the estimation of dynamic modulus of hot-mix asphalt. In spite of the successful performance of ANNs, they usually do not give a deep insight into the process which they use the available information to obtain a solution. In the present study, the approximation ability of one of the most widely used ANN architecture, namely multilayer perceptron (MLP) (Cybenko, 1989) is investigated. In order to provide a better form of relationships between input and output data, the derived MLP models are expressed in explicit forms.

Genetic programming (GP) (Banzhaf, Nordin, Keller, & Francone, 1998; Koza, 1992) is another alternative approach for the analysis of the rutting potential. GP may generally be defined as a supervised machine learning technique that searches a program space instead of a data space. Many researchers have employed GP and its variants to find out any complex relationships between the experimental data (e.g., Cevik & Cabalar, 2009; Cevik, 2007; Gandomi, Alavi, Kazemi, & Alinia, 2009; Johari, Habibagahi, & Ghahramani, 2006). Recently, Gandomi et al. (2010) developed new models to predict the flow number of asphalt mixtures utilizing gene expression programming. Also, Alavi, Ameri, et al. (2010); combined the GP and simulated annealing algorithms to obtain new prediction equations for the flow number of Marshall specimens. Multi expression programming (MEP) (Oltean & Dumitrescu, 2002) is a recent variant of GP using a linear representation of chromosomes. MEP has a special ability to encode multiple computer programs of a problem in a single chromosome. Applications of MEP to civil engineering tasks are quite new and restricted to a few areas (e.g., Alavi & Gandomi, in press; Alavi, Gandomi, Sahab, & Gandomi, 2010; Baykasoglu, Gullub, Canakci, & Ozbakir, 2008).

In this study, the MEP and MLP techniques are utilized to evaluate the rutting potential of dense asphalt mixtures in the form of the flow number. Generalized relationships were obtained to correlate the flow number to the particle size distribution of natural soil, bitumen, voids in mineral aggregate, Marshall stability, and Marshall flow. The proposed correlations were developed based on several uniaxial dynamic creep tests on standard Marshall specimens conducted at Iran University of Science and Technology civil engineering laboratories. The experimental database covers a wide range of aggregate gradation. A linear regression analysis was performed to benchmark the MEP and MLP-based correlations.

2. Rutting mechanisms characterization

Rutting can take place in different times of pavement service life. Basically, there are two mechanisms for rutting. The first mechanism that happens in the first years of pavement life is “initial rutting”. This mechanism is caused by the densification of asphalt mixture especially for loosely compacted pavements. The initial rutting is followed by the second mechanism called “shear deformation”. This mechanism, also named “secondary rutting”, is the primary mechanism of rutting in well compacted pavements. In the shear deformation stage, the material moves from under the wheel path and causes upheaval on the side. Previous studies indicated that the shear deformation was the primary rutting mechanism rather than the densification mechanism (Hofstra & Klomp, 1972; Sousa et al., 1991).

One of the tests that can characterize the mentioned mechanisms of rutting is the dynamic creep repeated load test. This test has widely been used to determine permanent deformation characteristics of paving material since it was employed by Monismith, Ogawa, and Freeme (1975) in the mid-1970s. The use of this test is a result of its simplicity and because of its logical connection with the permanent deformation in asphalt mixes. As with all other laboratory tests, one major problem with the laboratory creep tests are the difficulty in relating laboratory results with actual field performance (Tam, Solaimanian, & Kennedy, 2000). It is not feasible to directly predict the rut depth by use of the creep repeated load test. The most important output of the dynamic creep test is the curve of accumulated strain against number of load cycles which depends on the rutting resistance of mixture (Zhou et al., 2004) (see Fig. 1). The relationship between the accumulated strain and loading cycles can be explained by the densification and shear flow mechanisms (Alavi, Ameri, et al., 2010).

As shown in Fig. 1, the curve includes three distinct zones: (1) primary zone, (2) secondary zone, and (3) tertiary zone. During

the primary zone, the mixture volume decreases (densification) and accumulated strain increases dramatically. The secondary zone can be identified as a transition zone between the primary and the tertiary zones. The tertiary zone can be named as appearance of the second mechanism of rutting in which the shear deformation starts and rutting increases again. The three-stage permanent deformation behavior is a basic property of asphalt mixes (Zhou et al., 2004). According to Witczak's theory (Witczak et al., 2002), the loading cycle number where tertiary deformation starts is called the flow number. Reasonable correspondence of the permanent strain and flow number with the rut depth is shown by previous researchers. Besides the emphasis on the permanent strain, the experts generally agree on the flow number as the best indicator of the rutting potential of asphalt mixes (Alavi, Ameri, et al., 2010; Witczak et al., 2002; Zhou et al., 2004). The flow number is recorded where the minimum slope occurs in Fig. 1.

3. Experimental study

A comprehensive research study was conducted by NCHRP to develop a simple mechanical test to supplement the Superpave volumetric method of mixtures design. Among the five laboratory tests investigated, the dynamic creep test had very good correlation with measured rut depth and a high capability to estimate the rutting potential of asphalt layers (Kaloush & Witczak, 2002). On the basis of the results of the previous research (Alavi, Ameri, et al., 2010; Kaloush & Witczak, 2002), the dynamic creep test was chosen as an appropriate laboratory method to investigate the rutting potential of dense bituminous mixtures. Results of this experimental study were used in the development of the MEP and MLP-based models.

3.1. Testing apparatus

The uniaxial dynamic creep test has been used to determine the rutting potential of asphalt mixtures for many years. One of the devices developed on the basis of the dynamic creep test is universal testing machine (UTM). UTM-5 can be considered as the first generation of UTM. This device is capable of determining the important mechanical parameters of asphalt mixtures under similar field conditions (i.e. similar loading and temperature). The UTM-5 apparatus at Iran University of Science and Technology Asphalt Mixtures and Bitumen Research Center utilized for the aim of this study is shown in Fig. 2. This device is equipped with compressed air loading system and can impose any type of load such as rectangular and sinusoidal. The related software to the test has

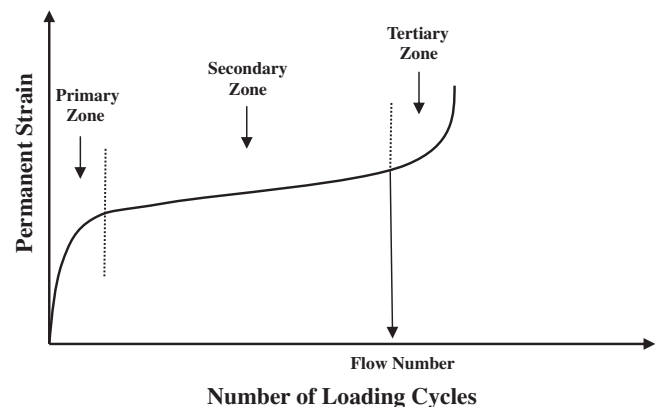


Fig. 1. Plot of accumulated strain versus number of loading cycles, obtained from dynamic creep test (Witczak et al., 2002).



Fig. 2. UTM-5 apparatus at Iran University of Science and Technology.

been developed in accordance with Australian Standard (AS 2891.12.1) and is in agreement with European, British and US Standards (King, 2003). A typical curve of accumulated strain versus loading cycles is as shown in Fig. 1.

3.2. Selected materials

The aggregates employed in the construction of asphalt samples were crushed aggregates and prepared from the gravel and sand mines of Rigzar Asphalt Factory located in the Shahryar road, Karaj, Iran. The used fillers were river materials and obtained from Makadam-e Shargh Asphalt Factory, Semnan, Iran. Also, bitumen with the penetration of 60/70 was supplied by Tehran Refinery and Pasarghad Oil Company, Tehran, Iran.

3.3. Grading of aggregate

Grading of aggregates can be characterized as one of the most effective factors on the resistance of asphalt mixtures against rutting. Poorly graded mixtures with too many fine or coarse aggregate would fail to provide the appropriate resistance to rutting.

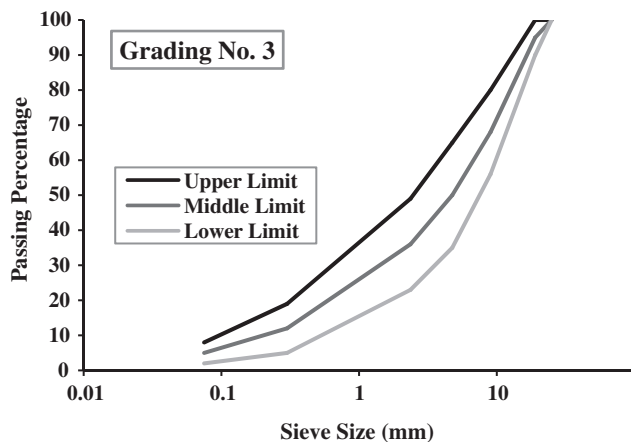


Fig. 3. Graph of 3 limits of grading No. 3.

In general, higher amount of fine aggregate as well as a perfect balance between the distribution of coarse aggregate, fine aggregate and filler may lead to increase in the resistance of asphalt sample (Alavi, Ameri, et al., 2010; Gandomi et al., 2010). In this research, 9 grading systems were considered for constructing the samples. Among different grading systems presented by Code 234 of Iran Management and Planning Organization (IAHC) (IAHC, 2000), upper, middle and lower limits of grading No. 3, 4 and 5 were selected. Figs. 3–5 show the grading diagram.

3.4. Aggregate tests

In order to control the quality of the aggregates, a number of tests such as Los Angeles abrasion and crushed percentage were conducted. The obtained results are presented in Tables 1 and 2.

3.5. Bitumen tests

The bitumen characteristics should be in accordance with the requirements specified in the standards. Thus, some tests such as penetration test, ductility test, and determination of softening

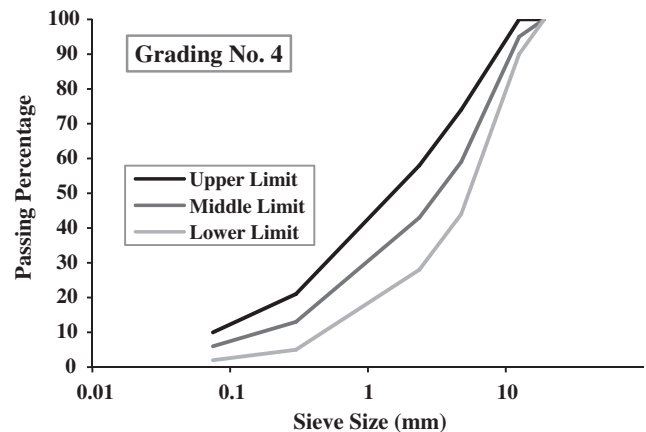


Fig. 4. Graph of 3 limits of grading No. 4.

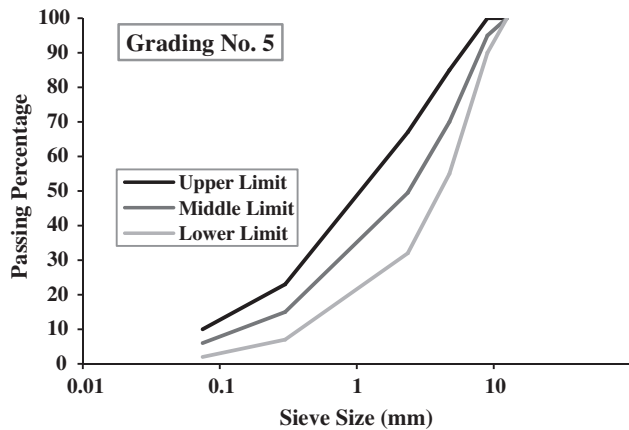


Fig. 5. Graph of 3 limits of grading No. 5.

point and unit weight of the bitumen were performed. The physical properties of the bitumen samples are given in Table 3.

3.6. Samples preparation

The asphalt mixture samples were fabricated and tested under the similar environmental conditions of field. The construction of the samples included three phases of separate heating of the aggregate and bitumen, mixing and compacting of the obtained mixture. The samples were constructed according to the Marshall method (ASTM D1559, 1993). The percentage of the used bitumen was selected in a way that the optimal amount of bitumen to be in the mean range of percentage. On the basis of the literature review and evaluation of executive documents (Alavi, Ameri, et al., 2010; Gandomi et al., 2010), the following bitumen percentages were adopted for the construction of the samples:

1. Grading No. 3: 4%, 4.5%, 5%, 5.5%, and 6%.
2. Grading No. 4: 4.5%, 5%, 5.5%, 6%, and 6.5%.
3. Grading No. 5: 5%, 5.5%, 6%, 6.5%, and 7%.

Finally, the compaction process was conducted using 75 blow of a 4.5 kg hammer to each side of the samples falling 45 cm (ASTM D1559, 1993). A total of 270 samples were constructed and tested in this research.

3.7. Tests on asphalt samples

After conducting the Marshall stability test on half of the samples, Rice test was performed to determine the percentage of the air void of the samples. VMA was determined using Eq. (1) and final VMA was obtained by taking the average of three samples (Tom & Krishna Rao, 2007, Chap. 26):

$$VMA = V_a + V_b, \quad (1)$$

where V_a is the air void of asphalt mixture; V_b is the volume percentage of the bitumen and can be determined using the following equation:

Table 1
Results of mineral aggregate tests.

Crushing percentage (1 side – 2 sides)	Los Angles abrasion test
ASTM D 5821	AASHTO T 96
92–100%	25%

Table 2

The specific gravity test results for coarse aggregate, fine aggregate and filler.

Aggregate range	Standard number	Specific gravity
Coarse aggregate (remained on sieve No. 8) (gr/cm ³)	ASTM C 127	2.49
Fine aggregate (passed from sieve No. 8 and remained on sieve No. 200) (gr/cm ³)	ASTM C 128	2.49
Fine aggregate (passed from sieve No. 200) (gr/cm ³)	ASTM C 188 – 95	2.60

Table 3

Results of tests on bitumen 60/70.

Tests	Standard number	Results
Penetration grade at 25 °C (1/10 mm)	ASTM D5	62
Ductility (cm)	ASTM D113	102
Softening point (°C)	ASTM D36	49
Unit weight at 25 °C (gr/cm ³)	ASTM D70	1.01

$$V_b = \frac{\frac{W_b}{G_b}}{\frac{W_1 + W_2 + W_3 + W_b}{G_m}}, \quad (2)$$

where W_1 , W_2 , W_3 are the weight of the coarse aggregate, fine aggregate and filler, respectively. W_b is the bitumen weight and G_b is the bitumen unit weight. G_m is the specific weight of the sample computed using:

$$G_m = \frac{W_m}{W_m - W_w}, \quad (3)$$

where W_m and W_w are respectively the weight of the asphalt sample in air and water. After conducting the dynamic creep tests on the samples, the flow numbers were determined. The final flow numbers were obtained by taking the average of three samples.

3.8. Repeated creep test results

The repeated creep test results have already been presented by the authors (Alavi, Ameri, et al., 2010; Gandomi et al., 2010). However, for more clarification, the outcomes of the experimental study are also presented herein in Figs. 6–8. The variations of the flow number (F_n) with bitumen percent (BP) for No. 3, 4 and 5 grading samples are shown in Fig. 6. It can be seen that, in most cases, F_n initially increases when BP increases to a certain point (optimum binder content) and then it starts decreasing. Besides, Fig. 6 indicates that the upper limits of grading No. 3, 4 and 5 have higher resistance to rutting compared to middle and lower limits. This is largely due to its higher amount of fine aggregate and better balance between distributions of materials. At each of the grading limits considered in this study, the percentage of VMA initially decreased. By plotting the curve of variations of VMA with F_n for each grading considered in this study (Fig. 7), it can be concluded that contrary to the growing-declining trend of VMA, F_n has a declining trend. This can be attributed to the increase of bitumen percent in the sample. In general, increase in the bitumen percent corresponds to increase in the rutting potential and softening of the sample. As shown in Fig. 7(a)–(c), among different limits of grading, the upper limits had the highest resistance to rutting. Fig. 8 illustrates the variations of F_n with Marshall stability to flow ratio (M/F) for different grading samples. It can be observed from this figure that F_n continuously increases with increasing M/F . The exception occurs at middle limit of grading No. 4. In

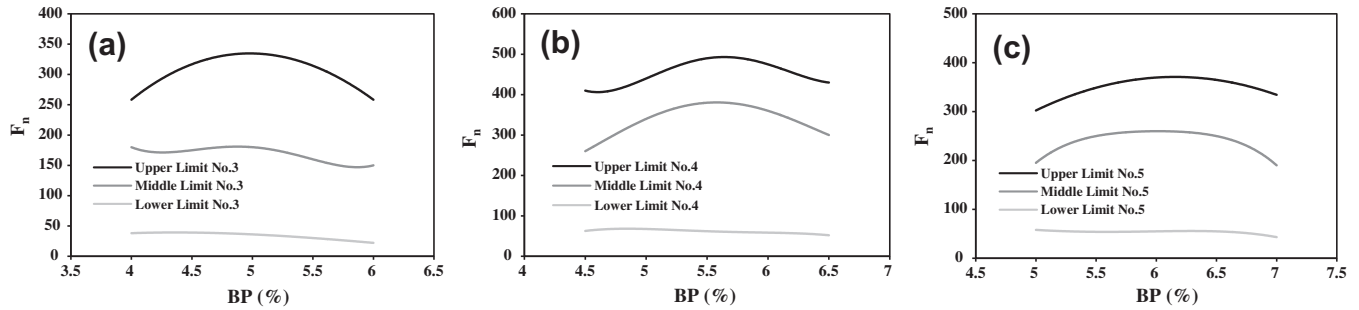


Fig. 6. The flow number variations versus bitumen percentage for grading No. 3, 4 and 5.

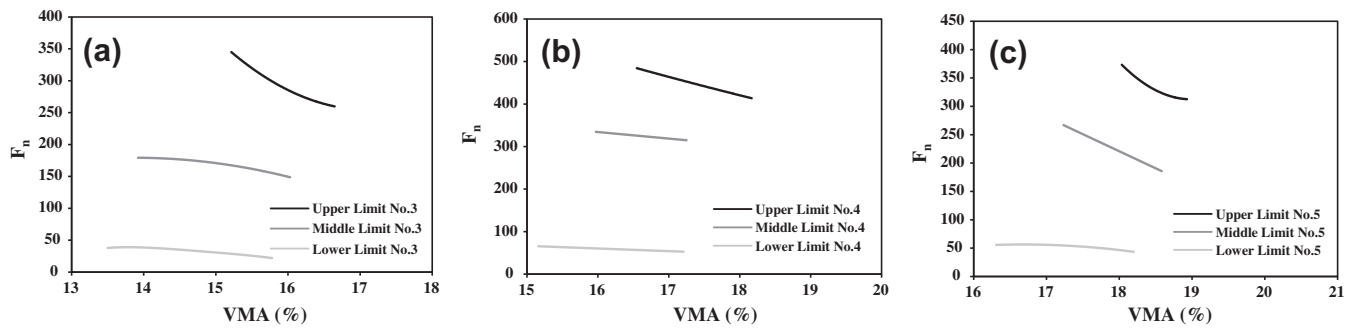


Fig. 7. The flow number variations versus VMA percentage for grading No. 3, 4 and 5.

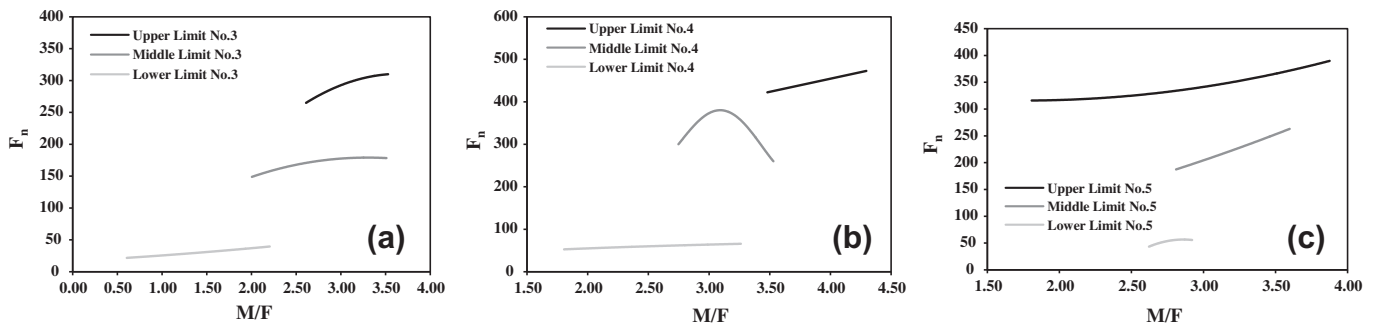


Fig. 8. The flow number variations versus M/F for grading No. 3, 4 and 5.

this case, the F_n increases with increasing M/F up to about 3 and then starts decreasing (Alavi, Ameri, et al., 2010; Gandomi et al., 2010).

4. Soft computing techniques

Soft computing includes evolutionary algorithms and all of their different branches combined with ANNs and fuzzy logic. Soft computing techniques have wide-ranging applications as important tools for approximating the nonlinear relationship between the model inputs and corresponding outputs. Developments in the computer hardware during the last two decades have made it much easier for these techniques to grow into more efficient frameworks. In addition, it has been proven that several soft computing techniques may be used as tools in problems where conventional approaches fail or perform poorly. A survey of the existing literature reveals the growing interest of the research community on the relatively new field of soft computing. In this paper, two of the soft computing techniques,

namely MEP and MLP are applied to the prediction of rutting resistance of asphalt mixtures.

4.1. Genetic programming

GP is a symbolic optimization technique that creates computer programs to solve a problem using the principle of Darwinian natural selection. GP was introduced by Koza (1992) as an extension of genetic algorithms (GAs). In GP, a random population of computer programs (trees) is created to achieve high diversity. A population member in GP is a hierarchically structured tree comprising functions and terminals. The functions and terminals are selected from a set of functions and a set of terminals. For example, the function set F can contain the basic arithmetic operations (+, −, ×, /, etc.), Boolean logic functions (AND, OR, NOT, etc.), or any other mathematical functions. The terminal set T contains the arguments for the functions and can consist of numerical constants, logical constants, variables, etc. The functions and terminals are chosen at random and constructed together to form a computer model in a tree-like structure with a root point with branches

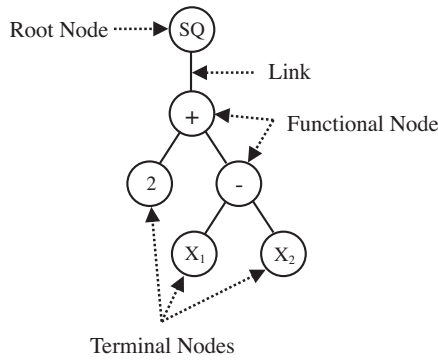


Fig. 9. The tree representation of a GP model $(2 + (X_1 - X_2))^2$.

extending from each function and ending in a terminal. An example of a simple tree representation of a GP model is illustrated in Fig. 9 (Alavi, Ameri, et al., 2010).

Creation of the initial population is a blind random search for solutions in the large space of possible solutions. Once a population of models has been created at random, the GP algorithm evaluates the individuals, selects individuals for reproduction, and generates new individuals by mutation, crossover, and direct reproduction (Koza, 1992). During the crossover procedure, a point on a branch of each solution (program) is selected at random and the set of terminals and/or functions from each program are then swapped to create two new programs as can be seen in Fig. 10. The evolutionary process continues by evaluating the fitness of the new population and starting a new round of reproduction and crossover (Alavi, Ameri, et al., 2010). During this process, the GP algorithm occasionally selects a function or terminal from a model at random and mutates it (see Fig. 11). MEP is a linear variant of GP. The linear variants of GP make a clear distinction between the genotype and the phenotype of an individual. Thus, the individuals are represented as linear strings that are decoded and expressed like non-linear entities (trees) (Gandomi, Alavi, & Sadat Hosseini, 2008; Oltean & Grossan, 2003a).

4.1.1. Multi expression programming

MEP is a subarea of GP that was developed by Oltean and Dumitrescu (2002). MEP uses linear chromosomes for solution encoding and has a special ability to encode multiple solutions (computer programs) in a single chromosome. Based on the fitness values of the individuals, the best encoded solution is chosen to represent the chromosome (Alavi, Gandomi, Sahab, et al., 2010).

Comparing to the other GP variants that store a single solution in a chromosome, MEP does not usually increase the complexity of the decoding process (Oltean & Grossan, 2003a). The evolutionary steady-state MEP algorithm starts by the creation of a random population of individuals. In order to evolve the best expression along a specified number of generations, two parents are selected using a binary tournament procedure and are recombined with a fixed crossover probability. Thereafter, two offspring are obtained by the recombination of two parents. The offspring are mutated and the worst individual in the current population is replaced with the best of them. This process is repeated until a termination condition is reached (Oltean & Grossan, 2003a).

MEP is represented similar to the way in which C and Pascal compilers translate mathematical expressions into machine code. The number of MEP genes per chromosome is constant and specifies the length of the chromosome. A terminal (an element in the terminal set T) or a function symbol (an element in the function set F) is encoded by each gene. A gene that encodes a function includes pointers towards the function arguments (Alavi, Gandomi, Sahab, et al., 2010). Function parameters always have indices of lower values than the position of that function itself in the chromosome. The first symbol in a chromosome must be a terminal symbol as stated by the proposed representation scheme. An example of an MEP chromosome can be seen below. It should be noted that numbers to the left stand for gene labels that do not belong to the chromosome. Using the set of arithmetic operators as $F = \{+, \times, /\}$ and the set of terminals as $T = \{x_1, x_2, x_3, x_4\}$, the example is given as follows:

- 0: x_1
- 1: x_2
- 2: $\times 0, 1$
- 3: x_3
- 4: $+ 2, 3$
- 5: x_4
- 6: $/ 4, 5$

The translation of MEP individuals into computer programs can be obtained by reading the chromosome top-down starting with the first position (Alavi, Gandomi, Sahab, et al., 2010). A terminal symbol defines a simple expression and each of function symbols specifies a complex expression obtained by connecting the operands specified by the argument positions with the current function symbol (Oltean & Grossan, 2003b). In the present example, genes 0, 1, 3 and 5 encode simple expressions formed by a single terminal symbol. These expressions are: $E_0 = x_1$; $E_1 = x_2$; $E_3 = x_3$; $E_5 = x_4$. Gene 2 indicates the operation “ \times ” on the operands located at positions

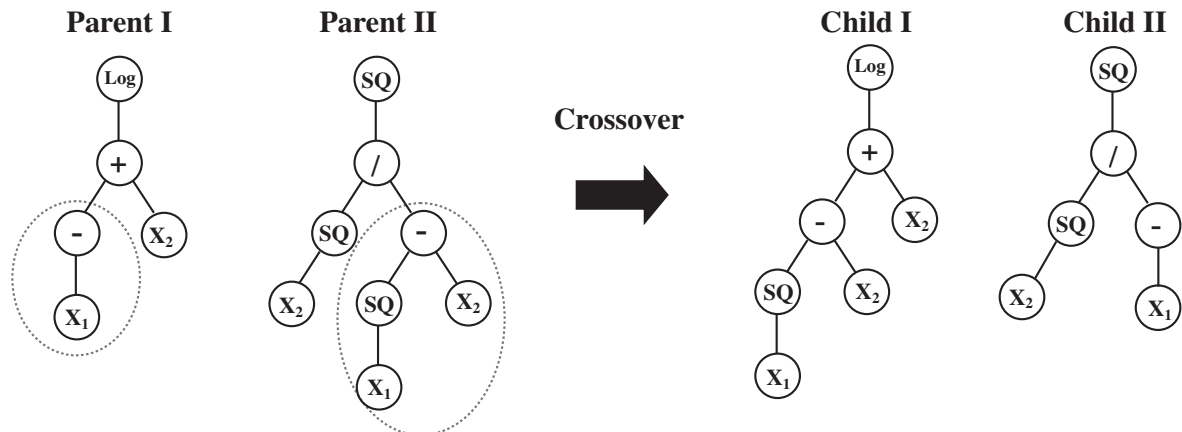


Fig. 10. Typical crossover operation in genetic programming.

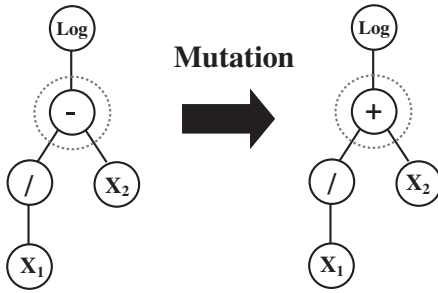


Fig. 11. Typical mutation operation in genetic programming.

0 and 1 of the chromosome. Therefore gene 2 encodes the expression: $E_2 = x_1 \times x_2$. Gene 4 indicates the operation “+” on the operands located at positions 2 and 3. Therefore gene 4 encodes the expression: $E_4 = (x_1 \times x_2) + x_3$. Gene 6 indicates the operation “/” on the operands located at positions 4 and 5. Therefore gene 6 encodes the expression: $E_6 = ((x_1 \times x_2) + x_3) / x_4$. In order to choose one of these expressions (E_1 – E_6) as the chromosome representer, multiple solutions in a single chromosome are encoded. Each of these expressions can be considered as a possible solution of a problem. The fitness of each expression encoded in an MEP chromosome is defined as the fitness of the best expression encoded by that chromosome. The fitness of an MEP chromosome may be computed by the following formula (Oltean & Grossan, 2003b):

$$f = \min_{i=1,m} \left\{ \sum_{j=1}^n |E_j - O_j^i| \right\}, \quad (4)$$

where n is the number of fitness cases, E_j is the expected value for the fitness case j , O_j^i is the value returned for the j th fitness case by the i th expression encoded in the current chromosome, and m is the number of chromosome genes.

4.2. Artificial neural network

ANNs are powerful tools for the prediction of nonlinearities using modeling philosophy similar to that used in the development of most of conventional statistical models. The conventional statis-

tical models use predefined mathematical equations to extract the relationships between the model inputs and corresponding outputs. Unlike most of the available statistical methods, ANNs use the data alone to determine the structure of the model and the unknown model parameters.

4.2.1. Multilayer perceptron network

MLPs are a class of ANN structures using feedforward architecture. MLPs are universal approximators, that is, they are capable of approximating essentially any continuous function to an arbitrary degree of accuracy (Cybenko, 1989). MLPs are usually applied to perform supervised learning tasks, which involve iterative training methods to adjust the connection weights within the network. They are usually trained with back propagation (BP) (Rumelhart, Hinton, & Williams, 1986) algorithm. Fig. 12 shows a schematic diagram of a BP neural network. An MLP network consists of an input layer, at least one hidden layer of neurons and an output layer. Each of these layers has several processing units and each unit is fully interconnected with weighted connections to units in the subsequent layer. Each layer contains a number of nodes. Every input is multiplied by the interconnection weights of the nodes (Alavi, Gandomi, Mollahasani, Heshmati, & Rashed, 2010). Finally, the output (h_j) is obtained by passing the sum of the product through an activation function as follows:

$$h_j = f \left(\sum_i x_i w_{ij} + b \right), \quad (5)$$

where $f()$ is activation function, x_i is the activation of i th hidden layer node and w_{ij} is the weight of the connection joining the j th neuron in a layer with the i th neuron in the previous layer, and b is the bias for the neuron. For nonlinear problems, the sigmoid functions (Hyperbolic tangent sigmoid or log-sigmoid) are usually adopted as the activation function. Adjusting the interconnections between layers will reduce the following error function:

$$E = \frac{1}{2} \sum_n \sum_k (t_k^n - h_k^n)^2, \quad (6)$$

where t_k^n and h_k^n are respectively the calculated output and the actual output value, n is the number of sample and k is the number

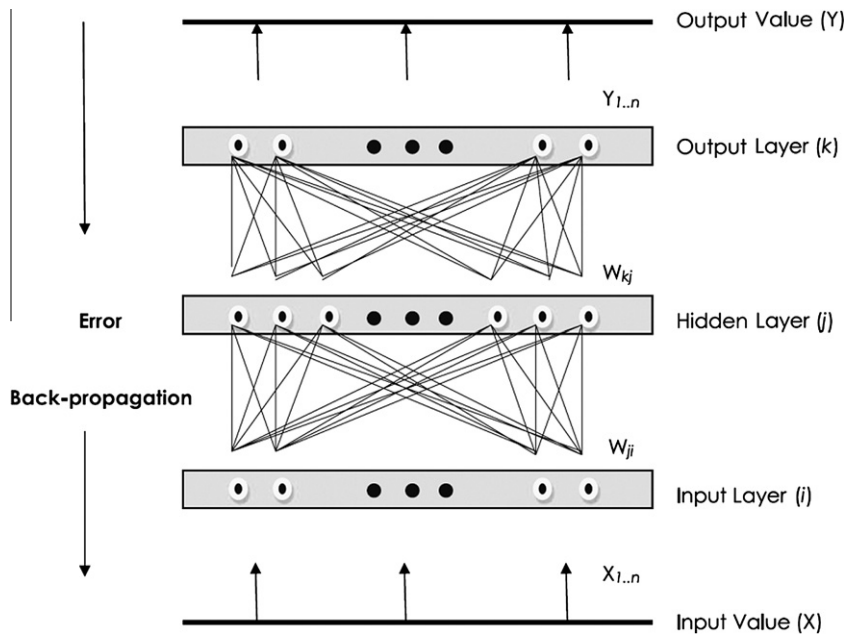


Fig. 12. A schematic diagram of a neural network using BP algorithm.

of output nodes. Further details of MLPs are provided by Cybenko (1989) and Alavi, Gandomi, Mollahasani, et al. (2010).

5. Development of models for rutting potential evaluation and analysis

Evaluation of the field rutting potential of asphalt mix has traditionally been a complicated task. Rutting is mainly influenced by several factors. An element of asphalt layer subjected to traffic loading transfers the load from the surface to underlying layers through intergranular contact and resistance to flow of the binder matrix. The stress pattern induced in a three-dimensional pavement structure due to traffic loading is complex. The stresses are transient and change with time as the wheel passes. When the response also depends on the time or on the rate of loading and temperature, material characterization becomes even more difficult. The properties of the individual components of asphalt and how they react with each other affect its behavior. There are occasions when the bituminous binder and aggregate are adequate but the mix fails to exhibit desired performance. The possible reasons are poor compaction, use of incorrect bituminous binder, poor adhesion, or some other problems associated with the mixture. In order to provide accurate assessment of the rutting potential of asphalt mix, the effects of several influencing factors should be incorporated into the model development. In the following subsections, first, the factors governing rutting potential are analyzed. Next, the details of developing the models are presented.

5.1. Analysis of internal factors affecting rutting

The internal factors affecting rutting can be divided into three basic categories of aggregate, bitumen and asphalt mixture characteristics (Alavi, Ameri, et al., 2010; Gandomi et al., 2010; Sousa et al., 1991).

5.1.1. Mineral aggregate

The mineral aggregates constitute the rate of 90–95% of mixture weight and 75–85% of mixture volume of asphalt mixtures and perform as skeleton and bearing member (Topal & Sengoz, 2005). Therefore, the physical and mineralogical properties of the mineral aggregate have noticeable effects on the quality and characteristics of asphalt mixtures. One of the most important parameters in aggregates is grading. Amount of the coarse aggregate, fine aggregate and nominal maximum aggregate size (NMAS) have remarkable influences on pavement rutting. From open grading to continuous grading, the rutting resistance increases which might be due to air void decline and more contact point at a certain compaction percentage (Sousa et al., 1991). Besides, the particle shape, being angular or rounded, and surface texture of aggregate, being rough or smooth, play an important role in the rutting resistance (Alavi, Ameri, et al., 2010).

5.1.2. Binder

The binder amount is one of the fundamental components of asphalt mixtures. It is used as a cohesive material to bond the aggregates. The rutting propensity of asphalt mixture is significantly affected by the stiffness of the binder. Many researchers have recognized the importance of the binder in contribution to the permanent deformation behavior of an asphalt aggregate mixture (Pardhan, 1995). With increase in the binder stiffness, mixture stiffens, and therefore, resistance to rutting increases (Sousa et al., 1991). The mixture with more amount of binder has more workability. Plasticity of such mixture increases at higher temperature and the mixture is more prone to rutting (Mahboub & Little, 1988). Based on the finite element simulation of asphalt samples,

an increase occurs in the rut depth by increasing the bitumen content (Pirabarooban, Zaman, & Tarefder, 2003).

5.1.3. Properties of asphalt mixture

Optimum amount of bitumen may have an appreciable influence on the capability of asphalt mixture to resist the permanent deformation (Sousa et al., 1991). The air voids of the mixture are negatively correlated with the asphalt binder content (Lavin, 2003). To prevent some difficulties such as lack of the stability and permanent deformation, the air void is recommended to be at least 3 percent (Monismith, Epps, & Finn, 1985). VMA is the total volume of voids within the mass the compacted aggregate. It is the volume of the air voids of the mixture plus the volume of the effective asphalt binder in the mixture. VMA allows room for enough asphalt binder to make a durable mixture plus enough room for the air voids to ensure a stable mixture [38]. In order to resist the permanent deformation, asphalt mixtures should have low percentage of VMA. Such grading can be determined using dry aggregate tests. It is widely known that the rutting resistance of the mixtures increases as the air void and VMA decrease (Pardhan, 1995; Sousa et al., 1991).

Stability is the most important property of asphalt mixtures in the wearing course design. It is the ability of the pavement to resist shoving and rutting under traffic. Thus, the stability should be high enough to handle traffic adequately, but not higher than the traffic conditions required. The lack of the stability in an asphalt mix causes unraveling and flow of the road surface. Flow is the ability of asphalt pavement to adjust to gradual settlements and movements in the subgrade without cracking. The flow is regarded as an opposite property to the stability. It determines the reversible behavior of the wearing course under traffic loads and affecting plastic and elastic properties of asphalt concrete (Hinischloglu & Agar, 2004; Kuloglu, 1999). The Marshall quotient is calculated as the ratio of the stability to the flow. This ratio is an indicator of the mix stiffness, resistance to the shear stress, permanent deformation, and rutting of the bitumen concrete (Haddadi, Ghorbel, & Laradi, 2008; Hinischloglu & Agar, 2004; Hitch & Russell, 1977; Nijboer, 1957). High Marshall quotient values imply high stiffness mix and therefore indicate a great ability of the mix to fail by cracking (Alavi, Ameri, et al., 2010).

5.2. Experimental database and data preprocessing

As mentioned previously, several uniaxial dynamic creep tests carried out in the laboratory environment utilizing UTM-5 to develop the database. This database has already been used by the authors (Alavi, Ameri, et al., 2010; Gandomi et al., 2010) to analyze the permanent deformation of asphalt mixtures. The database includes the measurements of coarse aggregate (C), fine aggregate (S), filler (FP), air voids (V_a), voids in mineral aggregate (VMA), bitumen (BP), Marshall stability (M), Marshall flow (F) and F_n . C/S , $FP(\%)$, $BP(\%)$, $VMA(\%)$ and M/F were considered as the input variables for the proposed models based on the analysis of the factors affecting rutting and after an extensive literature review. C/S and FP represent the grain size distribution, BP is a representative of the binder content, and VMA and M/F are the asphalt mixture characteristics. VMA is actually a property of aggregates in the mixture. Changes in the aggregates gradation or shape provide significant changes in VMA (Lavin, 2003). The descriptive statistics of the data used in this study are given in Table 4. The results of the repeated creep tests are given in Appendix A. To visualize the distribution of the samples, the data are presented by histogram plots (Fig. 13).

It is noteworthy that some of the above variables are fundamentally interdependent. This interdependency can cause problems in analysis as it will tend to exaggerate the strength of relationships between the variables. Filler is calculated by subtracting the sum

of coarse and fine aggregate from 100. Hence, filler and coarse aggregate to fine aggregate ratio were not used together in the proposed models. Out of the 270 samples constructed and tested herein, the final 118 flow number values were extracted by taking the average of three samples. For the MEP and MLP analyses, the developed database was randomly divided into learning, validation and testing subsets. The learning data were used for the training of the algorithm. The validation data were used to specify the generalization capability of the obtained models on the data that was not used for learning (model selection). The learning and validation data sets were used to select the best models and were included in the training process. Thus, they were categorized into one group referred to as “training data” (Alavi, Ameri, et al., 2010). In order to obtain a consistent data division, several combinations of the training and testing sets were considered. Out of the 118 data, 89 data were used as the training data (80 sets for the learning process and 9 sets as the validation data). The remaining 29 data sets were taken for the testing of the generalization capability of the MEP and MLP-based correlations on the data that played no role in building the models.

5.3. Performance measures

The following objective function (OBJ) was constructed as a measure of how well the model predicted output agrees with the experimentally measured output. The selections of the best MEP and MLP models were deduced by the minimization of the following function:

$$OBJ = \left(\frac{\text{No. Learning} - \text{No. Validation}}{\text{No. Training}} \right) \frac{MAE_{\text{Learning}}}{R_{\text{Learning}}^2} + \frac{2\text{No. Validation}}{\text{No. Training}} \times \frac{MAE_{\text{Validation}}}{R_{\text{Validation}}^2}, \quad (7)$$

where No. Learning , No. Validation and No. Training are respectively the number of learning, validation and training data; R and MAE are respectively correlation coefficient and mean absolute error given in the form of formulas as follows:

$$R = \frac{\sum_{i=1}^n (h_i - \bar{h}_i)(t_i - \bar{t}_i)}{\sqrt{\sum_{i=1}^n (h_i - \bar{h}_i)^2 \sum_{i=1}^n (t_i - \bar{t}_i)^2}}, \quad (8)$$

$$MAE = \frac{\sum_{i=1}^n |h_i - t_i|}{n}, \quad (9)$$

in which h_i and t_i are respectively actual and calculated outputs for the i th output, \bar{h}_i is the average of the actual outputs, and n is the number of sample. It is well known that only R is not a good indicator of prediction accuracy of a model. This is because that by shifting the output values of a model equally, the R value will not

change. The constructed objective function takes into account the changes of R and MAE together. Higher R values and lower MAE values result in lowering OBJ and, consequently, indicate a more precise model. In addition, the above function considers the effects of different data divisions for the learning and validation data.

5.4. Model construction using MEP

In some problems such as the rutting potential of asphalt mixtures, it is not simple to identify a relationship between the parameters, or the problem could be too complex to be described in a mathematical function. In this study, the MEP technique was employed to obtain meaningful relationships between the flow number of asphalt mixes and the factors affecting the mixture resistance to permanent deformation. The most important factors representing the rutting behavior were selected based on an extensive trial study and literature review. Consequently, the flow number (F_n) formulation was considered to be as follows:

$$\text{Log}(F_n) = f\left(\frac{C}{S}(\text{FP}), \text{BP}, \text{VMA}, \frac{M}{F}\right) \quad (10)$$

where,

C/S : Coarse aggregate to fine aggregate ratio

$\text{FP}(\%)$: Percentage of filler

$\text{BP}(\%)$: Percentage of bitumen

$\text{VMA}(\%)$: Percentage of voids in mineral aggregate

M/F : Marshall stability to flow ratio (Marshall quotient)

After developing and controlling several models with different combinations of the input parameters, two MEP-based models were selected and presented as the optimal models. The first combination includes C/S , BP , VMA and M/F , and the other comprises FP , BP , VMA and M/F . Various parameters involved in the MEP predictive algorithm are shown in Table 5. The parameter selection will affect the model generalization capability of MEP. They were selected based on some previously suggested values (Alavi & Gandomi, in press; Alavi, Gandomi, Sahab, et al., 2010; Baykasoglu et al., 2008) and also after a trial and error approach. For developing the MEP-based empirical models, source code of MEP (Oltean, 2004) in C++ was modified by the authors to be utilizable for the available problem. In order to evaluate the contribution of each predictor variable to the prediction of the flow number, frequency values of the input parameters were obtained. A frequency value equal to 1.00 for an input indicates that this input variable has been appeared in 100% of the best thirty programs evolved by MEP.

Table 4
Descriptive statistics of variables used in the model development.

Parameter	Input							Output
	C(%)	S(%)	FP(%)	BP(%)	VMA(%)	M(KN)	F(mm)	F_n
Mean	57.31	37.15	5.54	5.51	16.55	10.16	3.50	227
Standard error	1.32	1.04	0.29	0.07	0.13	0.19	0.06	13.25
Median	57.00	37.00	6	5.5	16.59	10.24	3.44	240
Standard deviation	14.33	11.31	3.17	0.81	1.41	2.04	0.62	143.97
Sample variance	205.33	128.01	10.06	0.66	2.00	4.15	0.38	20728.55
Kurtosis	-0.97	-0.83	-1.32	-0.81	-0.75	1.68	-0.73	-1.24
Skewness	-0.22	0.25	0.13	0.02	-0.24	-0.85	0.17	0.07
Range	48	39	9	3	5.84	12.57	2.65	488
Minimum	33	18	1	4	13.20	2.73	2.10	22
Maximum	81	57	10	7	19.04	15.30	4.75	510

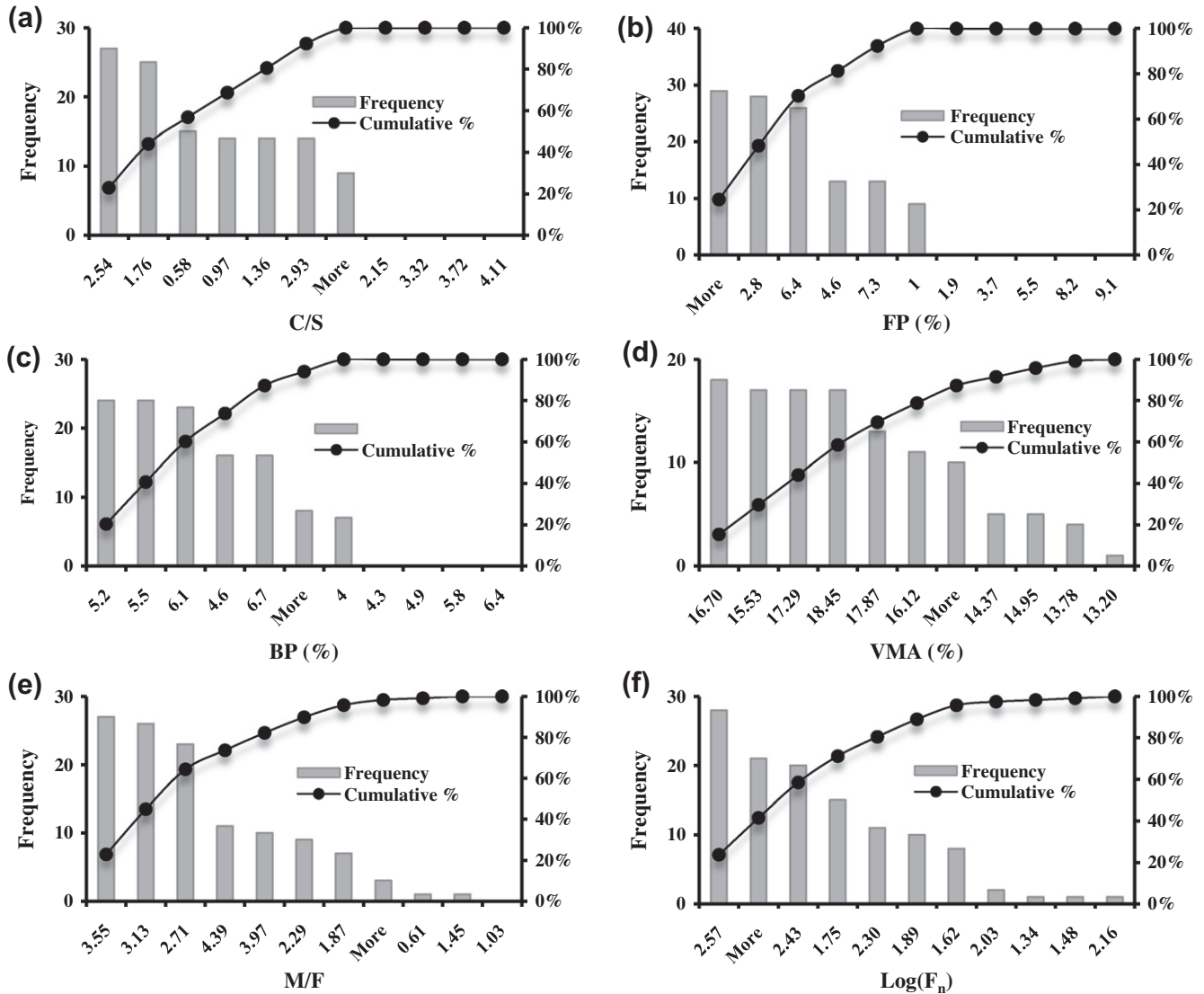


Fig. 13. The histograms of input and output variables.

5.4.1. The MEP-based formulation for the flow number of asphalt mix

The MEP-based formulations of the flow number, F_n , are as given below:

$$\text{Log}(F_n) = \frac{C/S}{(2C/S - 5)(-2VMA - 5)} + \frac{M/F}{(2C/S - 4)(BP - VMA)} + \text{Exp}\left(\frac{C/S - VMA + 1}{M/F - VMA - 4}\right) \quad (11)$$

$$\text{Log}(F_n) = \frac{-4FP - BP^2}{VMA \times \text{Exp}(FP)} + \frac{FP + 2VMA + 1/M/F}{VMA} \quad (12)$$

A comparison the experimental and predicted flow number values for the training and testing data is shown in Fig. 14. The frequency values of input parameters are presented in Fig. 15. According to these figures, the flow number is more sensitive to VMA, C/S and FP compared with the other inputs.

5.5. Model construction using MLP

After developing and controlling several models with different combinations of the input parameters, two MLP-based models

were selected and presented as the optimal models. Similar to the MEP models, the predictor variables in the first MLP model were C/S, BP, VMA and M/F; those of the second model were FP, BP, VMA and M/F. For the development of ANN models, a script was written in the MATLAB environment using Neural Network Toolbox 5.1. The performance of an ANN model mainly depends on the network architecture and parameter settings. For traditional MLP, a single hidden layer network is sufficient to uniformly

Table 5
Parameter settings for the MEP algorithm.

Parameter	Settings
Function set	+, -, ×, /, exp, sin, cos
Number of generations	100
Population size	500 – 2000
Chromosome length	50 Genes
Number of generations	250
Crossover probability	0.5, 0.9
Crossover type	Uniform
Mutation probability	0.01
Terminal set	Problem inputs

approximate any continuous and nonlinear function according to a universal approximation theorem, demonstrated concurrently by several researchers (e.g., Alavi, Gandomi, Mollahasani, et al., 2010; Cybenko, 1989). Choice of the number of the hidden layers, hidden nodes, learning rate, epochs and type of activation function plays an important role in model construction. Hence, several MLP network models with different settings for the mentioned characters were trained to reach the optimal configurations with desired precision (Eberhart & Dobbins, 1990). Also, hyperbolic tangent sigmoid and quasi-Newton back-propagation were respectively adopted as the transfer function and training algorithm.

ANN toolbox in MATLAB randomly assigns the initial weights and biases for each run each time (MathWorks Inc, 2007). These assignments considerably change the performance of a newly trained ANN even all the previous parameter settings and ANN architecture are kept constant. This leads to extra difficulties in the selection of optimal ANN architecture and parameter settings. To overcome this difficulty the weights and biases were frozen after the network was well trained and then the trained ANN models translated into explicit forms (Alavi, Gandomi, Mollahasani, et al., 2010; Guzelbey et al., 2006; Tapkin et al., 2009). For brevity, detailed explanations of the procedure used to convert the ANN models into simple equations are not given. Relative importance values of the various inputs of the proposed separate models were

calculated using Garson's algorithm (Garson, 1991). According to this algorithm, the input-hidden and hidden-output weights of the trained ANN models are partitioned and the absolute values of the weights are taken to calculate the relative importance of the input variables.

5.5.1. The MLP-based formulation for the flow number of asphalt mix

The model architecture that gave the best results for the formulation of the flow number in terms of C/S, BP, VMA and M/F was found to contain:

- One invariant input layer, with 4 ($n = 4$) arguments.
- One invariant output layer with 1 node providing the value of $\text{Log}(F_n)$.
- One hidden layer having 7 ($m = 7$) nodes.

The explicit formulations of F_n is as follows:

$$\text{Log}(F_n) = \frac{2}{1 + e^{-2\left(B^h + \sum_{j=1}^m \tanh(F_j) \times W_{lj}^h\right)}} - 1, \quad (13)$$

where,

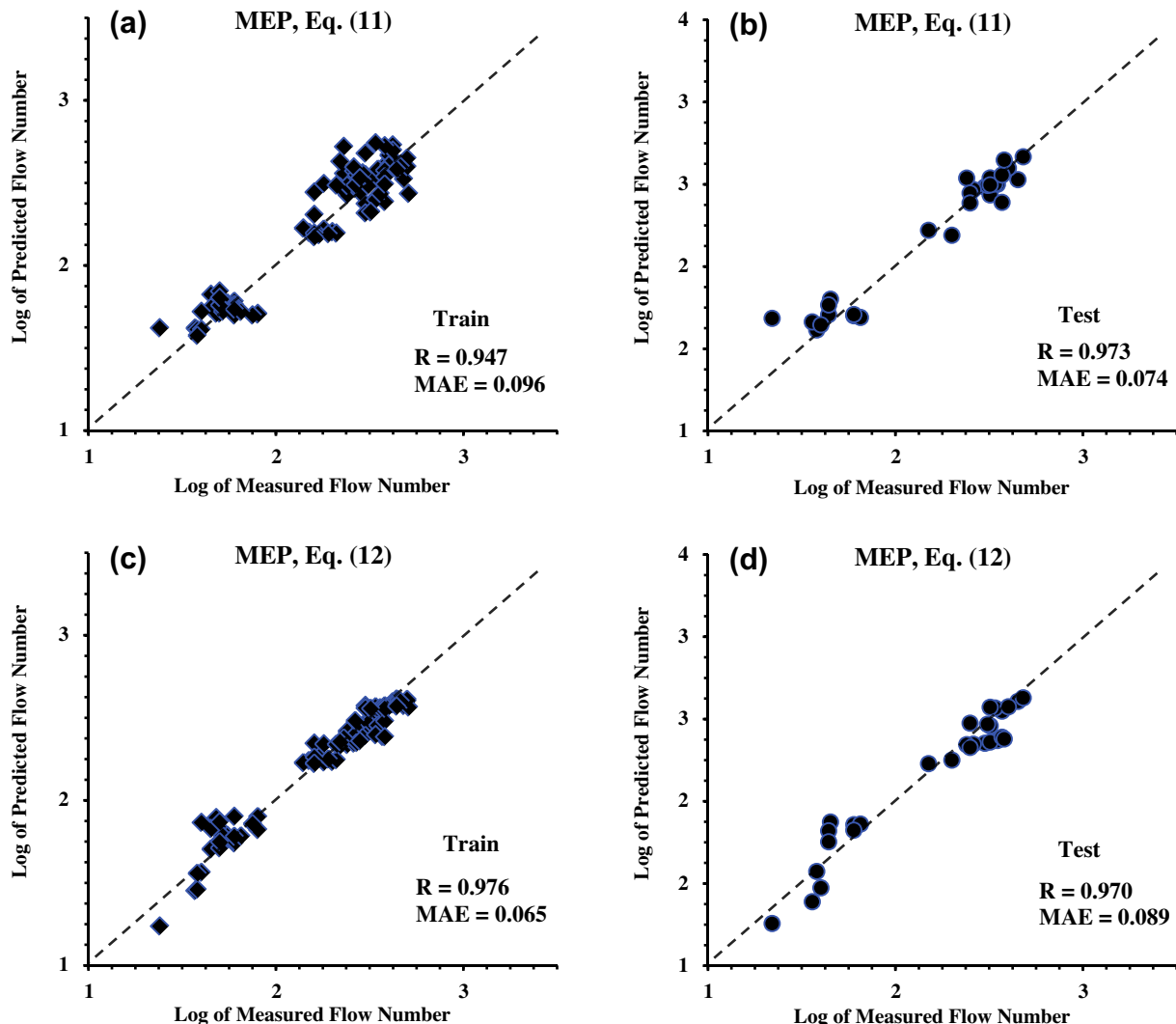


Fig. 14. Experimental versus predicted flow number using the MEP models.

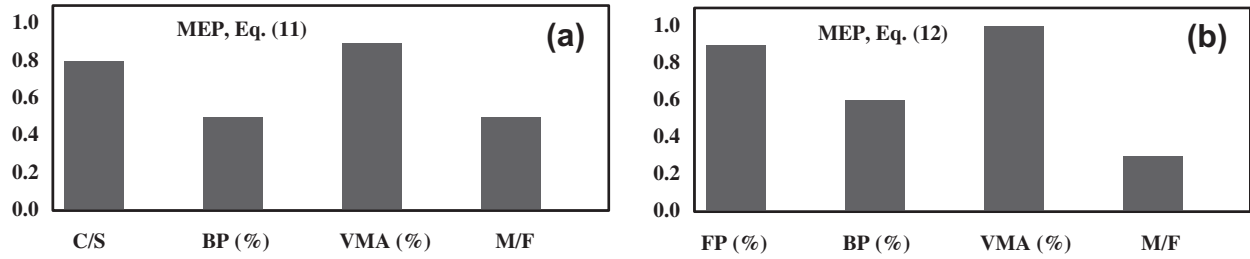


Fig. 15. Frequency values of the input parameters.

$$F_j = \sum_{k=1}^n X_n W_{kj}^i + Bias = \frac{C}{S} \times W_{1j}^i + BP \times W_{2j}^i + VMA \times W_{3j}^i + \frac{M}{F} \times W_{4j}^i + B_j^i, \quad j = 1, \dots, m, \quad (14)$$

where, $\text{Log}(F_n)$, C/S , BP , VMA and M/F are the variables that were normalized using the well-known linear normalization method (Mollahasani, Alavi, Gandomi, & Rashed, in press). The input layer weights (W^i), input layer biases (B^i), hidden layer weights (W^h) and hidden layer bias (B^h) of the optimum MLP model are as follows:

$$2 [W^i] = \begin{bmatrix} 4.996 & 2.169 & -5.524 & -6.203 \\ 1.252 & 3.245 & -1.117 & -0.506 \\ -17.136 & -6.376 & -13.213 & 2.522 \\ -4.002 & -7.173 & 5.358 & 2.561 \\ -4.076 & -2.410 & 5.885 & 6.841 \\ 1.200 & -0.214 & 0.128 & 0.189 \\ -4.451 & 5.719 & -5.160 & -2.354 \end{bmatrix}_{m \times n} \quad (15)$$

$$[B^i] = \begin{bmatrix} 0.636 \\ -1.058 \\ -7.437 \\ 0.631 \\ -0.652 \\ 0.203 \\ -2.354 \end{bmatrix}_{m \times 1} \quad (16)$$

$$[W^h] = [1.328 \quad -0.299 \quad 0.202 \quad -0.158 \quad 1.215 \quad -0.818 \quad 0.122]_{1 \times m} \quad (17)$$

$$[B^h] = [0.118] \quad (18)$$

The model architecture that gave the best results for the formulation of the flow number in terms of FP , BP , VMA and M/F was found to contain:

- One invariant input layer, with 4 ($n = 4$) arguments;
- One invariant output layer with 1 node providing the value of $\text{Log}(F_n)$.
- One hidden layer having 9 ($m = 9$) nodes.

The explicit formulations of F_n is as given below:

$$\text{Log}(F_n) = \frac{2}{1 + e^{-2(B^h + \sum_{j=1}^m \tanh(F_j) \times W_{1j}^h)}} - 1 \quad (19)$$

where,

$$F_j = \sum_{k=1}^n X_k W_{kj}^i + Bias = FP \times W_{1j}^i + BP \times W_{2j}^i + VMA \times W_{3j}^i + \frac{M}{F} \times W_{4j}^i + B_j^i, \quad i = 1, \dots, m \quad (20)$$

in which, $\text{Log}(F_n)$, F , BP , VMA and M/F are the variables normalized using the well-known linear normalization method (Mollahasani et al., in press). The optimum weights matrices (W^i) and (W^h) and bias vectors, (B^i) and (B^h), are presented below:

$$[W^i] = \begin{bmatrix} -1.038 & -0.710 & 6.222 & 1.198 \\ 4.891 & 3.196 & 7.698 & 2.370 \\ -6.851 & -8.642 & 3.527 & -0.037 \\ -0.877 & 1.209 & -1.414 & -11.171 \\ 0.825 & 1.333 & 5.575 & 2.634 \\ 4.157 & 0.162 & -0.863 & 0.442 \\ 5.884 & 2.924 & -5.916 & 8.198 \\ 4.587 & 1.226 & -4.565 & 3.085 \\ -8.653 & -4.402 & 3.920 & 0.876 \end{bmatrix}_{m \times n}, \quad (21)$$

$$[B^i] = \begin{bmatrix} -1.860 \\ 0.709 \\ 0.770 \\ 4.613 \\ -3.196 \\ 4.219 \\ -5.415 \\ -0.016 \\ -2.265 \end{bmatrix}_{m \times 1}, \quad (22)$$

$$[W^h] = [-0.178 \quad 0.182 \quad 0.139 \quad 0.145 \quad 0.192 \quad 3.255 \quad 0.191 \quad 0.134 \quad -0.134]_{1 \times m}, \quad (23)$$

$$[B^h] = [-2.959]. \quad (24)$$

Both of the MLP models were built with a learning rate of 0.05 and trained for 1000 epochs. A comparison of the actual and predicted flow number for the training and testing data sets is shown in Fig. 16. The relative importance values of the input parameters are presented in Fig. 17. As it is seen, the flow number is more sensitive to C/S , F and VMA in comparison with the other effective parameters.

5.6. Model construction using regression analysis

In the conventional material modeling process, regression analysis is an important tool for building a model. In this study, a multivariable least squares regression (MLSR) (Ryan, 1997) analysis

was performed to have an idea about the predictive power of the MEP and MLP techniques, in comparison with a classical statistical approach. The LSR method is extensively used in regression analysis primarily because of its interesting nature. LSR minimizes the sum-of-squared residuals for each equation, accounting for any cross-equation restrictions on the parameters of the system. If there are no such restrictions, this technique is identical to estimating each equation using single-equation ordinary least squares.

The LSR models were developed using the same input variables as MEP and MLP. Eviews software package (Maravall & Gomez, 2004) was used to perform the regression analysis.

5.6.1. The MLSR-based formulation for the flow number of asphalt mix

The formulations of the flow number, F_n , in terms of C/S, FP(%), BP(%), VMA(%), and M/F for the best result by the MLSR analysis are as given below:

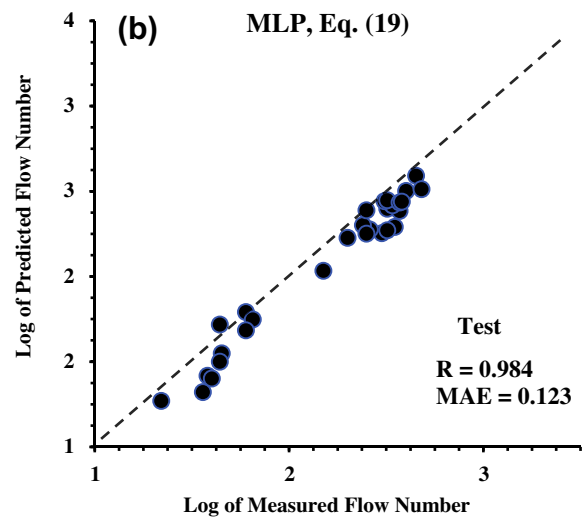
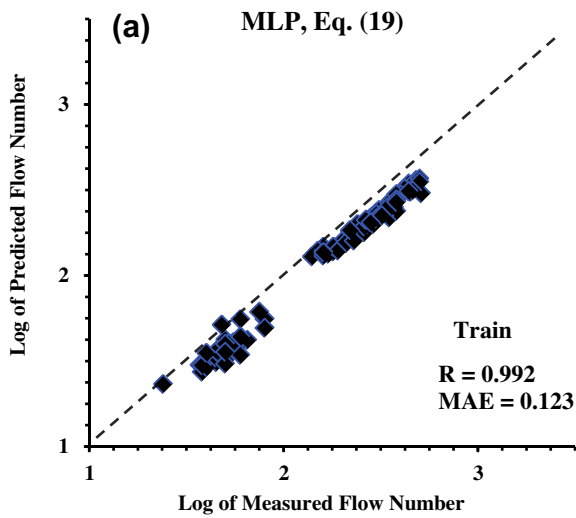
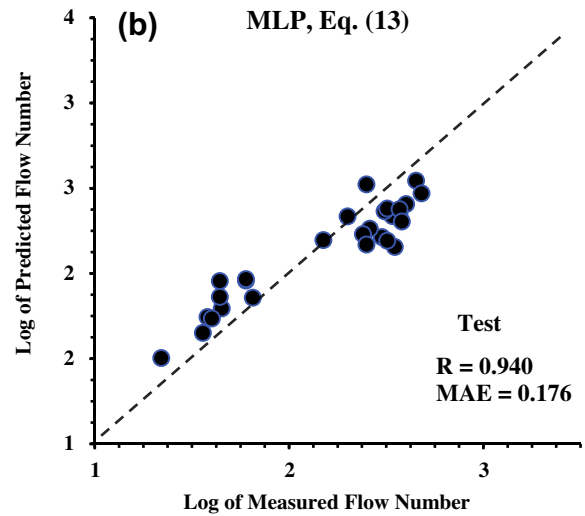
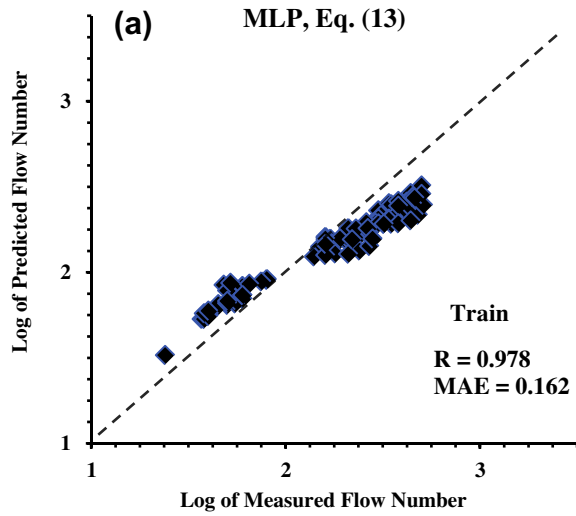


Fig. 16. Experimental versus predicted flow number using the MLP models.

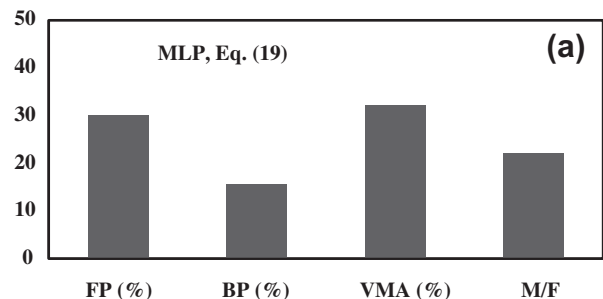
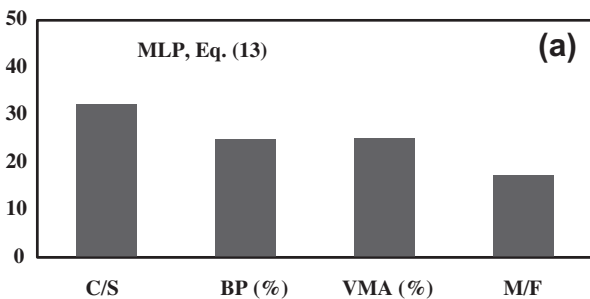


Fig. 17. Relative importance of the input parameters.

$$\begin{aligned} \text{Log}(F_n) = & -0.4893 \frac{C}{S} - 0.0042 \text{BP} - 0.1511 \text{VMA} \\ & - 0.0639 \frac{M}{F} + 5.7907, \end{aligned} \quad (25)$$

$$\begin{aligned} \text{Log}(F_n) = & 0.1200 \text{FP} + 0.05089 \text{BP} - 0.0626 \text{VMA} \\ & + 0.0516 \frac{M}{F} + 2.1584. \end{aligned} \quad (26)$$

6. Comparison of the rutting potential predictive models

As described above, four different formulas were obtained for the assessment of the flow number of asphalt mixtures by means of MEP and MLP. Overall performance of the MEP, MLP and MLSR-based models on the whole of data are summarized in Table 6. Comparisons of the flow number predictions obtained by these models are also visualized in Fig. 18. No rational model to predict the flow number of asphalt mixes has been developed yet that would encompass the influencing variables considered in this

Table 6
Overall performances of the proposed models for flow number prediction.

Model	Performance	
	R	MAE
MEP, Eq. (11)	0.954	0.091
MEP, Eq. (12)	0.974	0.071
MLP, Eq. (13)	0.965	0.166
MLP, Eq. (19)	0.990	0.123
MLSR, Eq. (25)	0.920	0.117
MLSR, Eq. (26)	0.932	0.120

study. Therefore, it was not possible to conduct a comparative study between the results of this research and those of previous studies.

Comparing the performance of the proposed relationships, it can be seen from Figs. 15 and 16, and Table 6 that Eq. (19) of MLP has produced the best (higher) R values on the training, testing and whole of data. The best (lowest) MAE values on the training and entire database are provided by Eq. (12) evolved by MEP. Considering the MAE values on the testing data, Eq. (11) of MEP performs superior than the other models. The equations obtained by means of the MLP method are very complex. These models are appropriate to be used as a part of a computer program or via spreadsheet programming. On the other hand, the MEP-based equations are really short, simple and can be used for routine design practice via hand calculations. In general, the MEP and MLP-based formulas perform superior than the MLSR models developed with the same variables as inputs. Overall, the models which have taken into account the effects of FP as input variable outperform those using C/S. Although most of the proposed regression-based models yield good results for the current database, empirical modeling based on statistical regression techniques has significant limitations. Most commonly used regression analyses can have large uncertainties. It has major drawbacks pertaining idealization of complex processes, approximation and averaging widely varying prototype conditions (Alavi, Ameri, et al., 2010).

7. Parametric analysis

For further verification of the models, a parametric analysis was performed in this study. The main goal is to find the effect of each parameter on the flow number (F_n). Fig. 19 presents the predicted values of the flow number obtained by the proposed MEP and

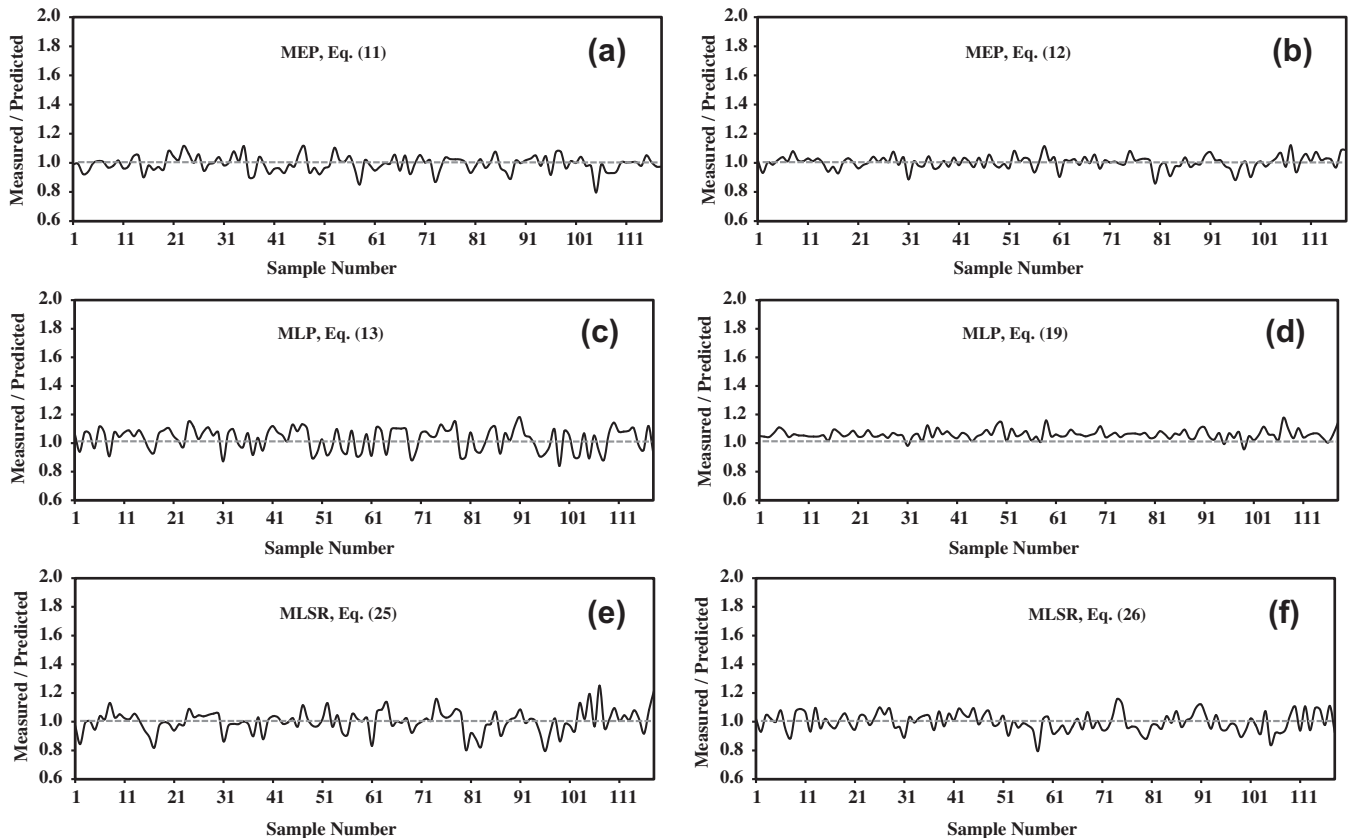


Fig. 18. A comparison of the ratio between the experimental and predicted flow number values using different models.

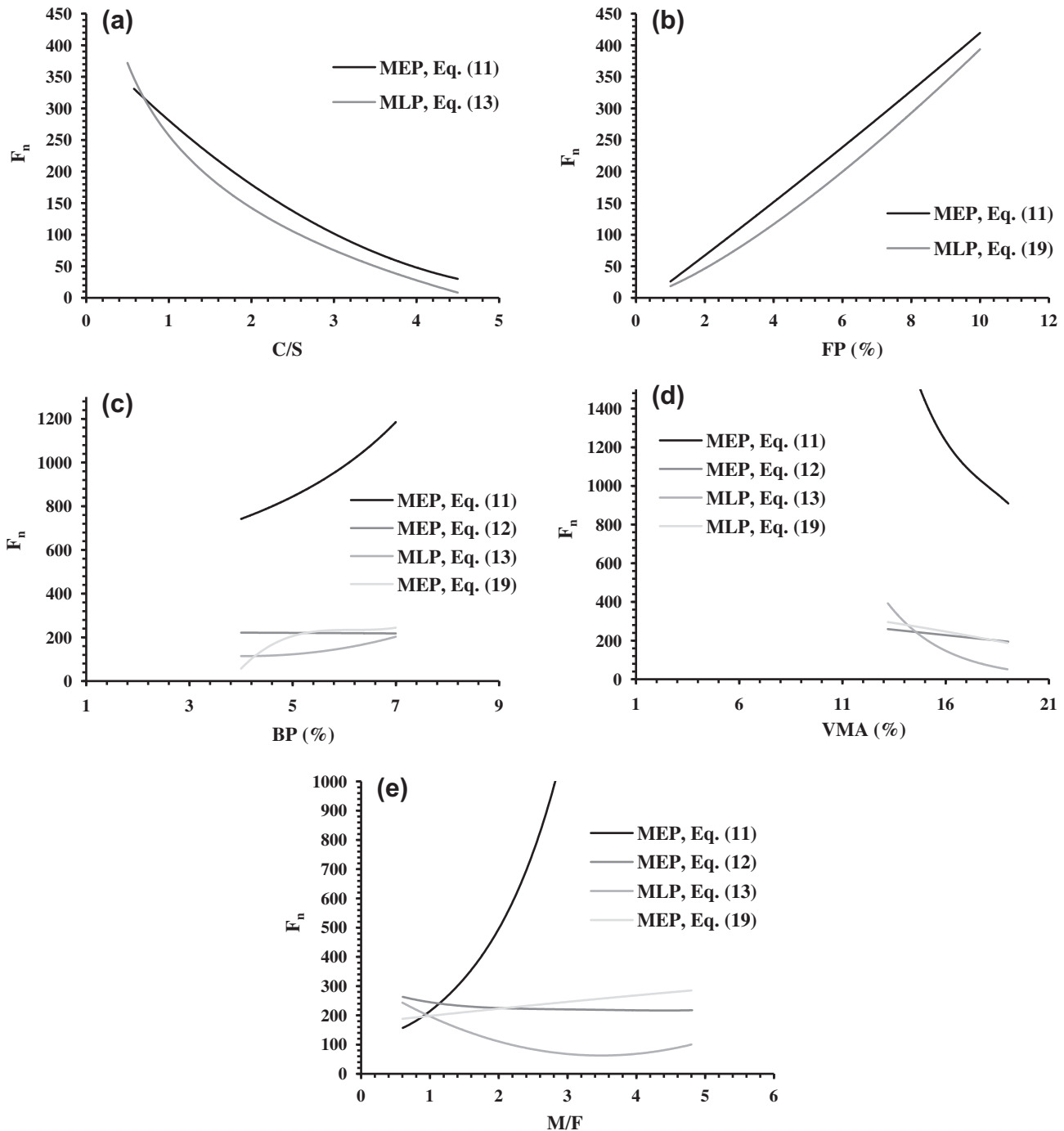


Fig. 19. Parametric analysis of the flow number in the MEP and MLP-based models.

MLP-based correlations as a function of each parameter. The tendency of the F_n predictions to the variations of C/S, FP (%), BP (%), VMA (%), and M/F can be determined according to these figures.

As can be seen in Fig. 19(a) and (b), F_n continuously decreases due to increasing C/S and increases with increasing FP. This is an expected case from a pavement engineering viewpoint. A designer can select various aggregate properties to give an asphalt mixture with high or low Marshall stability. Any material that can stiffen an asphalt mixture will also increase the Marshall stability. It is well known that increase in the fine aggregate and filler content will stiffen the total asphalt mixture, leading to higher Marshall stability values and better resistance to the permanent deformation. This is mainly due to the fact that the air void between the aggregates is

filled by the fine aggregate and filler and consequently, a more integrate grading will be obtained. The fine aggregate and filler provide the load spreading characteristics of the mixture. The above results are in acceptable agreement with the obtained experimental trends. As shown in Figs. 6–8, the upper limits of the grading No. 3, 4 and 5 with higher amount of the fine particles provide higher flow number and lower rutting potential compared with the middle and lower limits of each grading with lower fine particles.

In Fig. 19(c), one can see that F_n initially increases when BP increases. It seems that the MEP and MLP models are capable of capturing the variations of F_n with increasing BP up to the optimum binder content, which is a growing trend as previously shown in

Fig. 6. As the VMA values increase, the specimens become less resistant to the applied loads. Therefore, from the nature of asphalt, accumulated strains at the end of repeated creep test tend to increase resulting in decreased F_n . This can be attributed to the increase of the bitumen percent in the sample. In general, increase in the bitumen percent corresponds to increase in the rutting potential and softening of the sample. This is verified completely by the proposed MEP and MLP models as shown in Fig. 19(d). The results of the experimental study and also several other studies indicate that resistance against the permanent deformation increases as VMA decreases (e.g., Lavin, 2003; Pardhan, 1995; Sousa et al., 1991).

As can be seen in Fig. 19(e), the effect of M/F on the rutting potential of asphalt mixtures is more complex than the effect of other variables. M/F is the ratio of stability to flow and represents the ratio of load to deformation. This ratio may be used to give an indicator of the mixture stiffness while specifying a minimum flow value may prevent mixtures susceptible to embrittlement being used. Based on the previous studies, a higher M/F value indicates a high stiffness mix with a greater ability to spread the applied load. Therefore, the pavements being more resistant to the permanent deformation are obtained (Hinischoglu & Agar, 2004; Lavin, 2003; Nicholls, 1998; Nijboer, 1957; Zoorob & Suparna, 2000). However, there is no clear consensus in the literature about the effect of M/F increment on the rutting resistance of asphalt mixtures. Recently, Tayfur, Ozen, and Aksoy (2007) investigated the rutting performance of asphalt mixtures containing polymer modifiers. It was found that M/F may not be a good indicator for measuring of the permanent deformation. The results of the parametric study for M/F obtained by MEP, Eq. (11) and MLP, Eq. (19) indicate that F_n increases with increasing M/F . The relevant results for Eq. (12) of MEP indicate that F_n is negatively correlated with M/F . The results for Eq. (13) of MLP show that F_n initially decreases when M/F increases up to about 3.5 and thereafter it starts increasing.

8. Conclusions

In this study, a robust variant of GP, namely MEP and MLP of ANNs were utilized to assess the flow number of asphalt-aggregate mixtures. Four different correlations were developed for the flow number prediction using different combinations of the affecting parameters. On the basis of an extensive trial study and literature review, the coarse aggregate to fine aggregate ratio (C/S), filler (FP), bitumen (BP), voids in mineral aggregate (VMA), and Marshall quotient (M/F) were identified to be used as the predictor variables. Several uniaxial dynamic creep tests were carried out on standard Marshall specimens in the laboratory environment to develop a

comprehensive database. The MEP and MLP-based correlations were benchmarked against the multivariable linear regression models. The following conclusions can be derived from the results presented in this research:

- (i) It was observed that the MEP and MLP-based correlations are capable of predicting the flow number of asphalt mixtures with high accuracy. Due to nonlinearity in rutting behavior, the nonlinear MEP and MLP models produced better outcomes over the developed linear regression-based models.
- (ii) The proposed models simultaneously take into account the role of several important factors representing the rutting behavior. Better performance of the correlations developed using FP instead of C/S implies the necessity of using FP for the performed MEP and MLP analyses.
- (iii) The developed generalized correlations can be used for routine design practice in that they were derived from tests on mixtures with a wide range of aggregate gradation and properties. The MEP-based formulas are much simpler than the MLP equations.
- (iv) A major advantage of MEP and MLP for determining the flow number lies in their powerful ability to model the mechanical behavior without any prior assumptions.
- (v) The contribution of each input parameter in the MEP and MLP models was evaluated through a sensitivity analysis. C/S , F and VMA were found to be more effective to explain the variations of the flow number compared with the other mixture properties.
- (vi) In the MEP and MLP-based modeling, the effects of different aggregate gradation properties are concurrently incorporated into the model development and analyzed. Hence, unlike experimental design procedures, there is no need to consider different grading systems such as upper, middle and lower limits.
- (vii) By employing the MEP and MLP approaches, the flow number can accurately be estimated without carrying out sophisticated laboratory tests with UTM or any similar testing equipment.
- (viii) As more data become available, including those for other types of asphalt mixtures and test conditions, the proposed models can be improved to make more accurate predictions for a wider range.

Appendix A

See Table 7.

Table 7
The repeated creep test results on the asphalt samples.

Test No.	C(%)	S(%)	F(%)	BP(%)	V_a (%)	VMA(%)	M(kN)	F(mm)	F_n
1	55	38	7	4	7.69	16.30	11.74	3.27	260
2	55	38	7	4	7.52	16.16	9.49	2.90	350
3	55	38	7	4.5	5.60	15.45	11.58	3.40	300
4	55	38	7	4.5	5.67	15.51	11.42	3.72	310
5	55	38	7	5	4.55	15.54	11.38	3.73	310
6	55	38	7	5	4.08	15.12	12.88	3.80	340
7	55	38	7	5	3.93	14.99	15.30	3.68	380
8	55	38	7	5.5	3.86	15.95	12.70	4.75	320
9	55	38	7	5.5	2.89	15.10	12.49	4.23	265
10	55	38	7	5.5	3.83	15.92	12.60	3.66	350
11	55	38	7	6	3.90	16.99	11.44	4.32	280
12	55	38	7	6	4.39	17.42	11.30	3.95	240
13	55	38	7	6	2.17	15.50	11.20	4.73	250
14	68	28	4	4	5.21	14.05	11.52	3.28	170

(continued on next page)

Table 7 (continued)

Test No.	C(%)	S(%)	F(%)	BP(%)	V _a (%)	VMA(%)	M(kN)	F(mm)	F _n
15	68	28	4	4	5.36	14.19	10.80	3.30	160
16	68	28	4	4.5	4.60	14.54	12.40	3.76	190
17	68	28	4	4.5	4.34	14.31	12.35	3.64	160
18	68	28	4	5	3.42	14.52	11.51	4.38	200
19	68	28	4	5	3.64	14.72	11.39	4.16	210
20	68	28	4	5	3.87	14.92	11.59	4.11	150
21	68	28	4	5.5	3.53	15.65	10.35	4.30	140
22	68	28	4	5.5	2.93	15.13	10.74	4.32	200
23	68	28	4	5.5	3.28	15.43	9.88	4.25	180
24	68	28	4	6	1.71	15.09	12.90	4.63	160
25	68	28	4	6	2.14	15.46	8.99	4.44	150
26	68	28	4	6	4.56	17.55	5.02	4.35	160
27	81	18	1	4	4.28	13.20	8.57	4.56	38
28	81	18	1	4	4.68	13.56	7.96	3.48	40
29	81	18	1	4	4.89	13.74	8.86	4.32	38
30	81	18	1	4.5	4.24	14.20	9.38	4.16	40
31	81	18	1	4.5	3.68	13.70	9.86	4.20	37
32	81	18	1	4.5	3.74	13.76	9.07	4.48	38
33	81	18	1	5	3.86	14.90	8.31	4.65	36
34	81	18	1	5.5	2.05	14.33	6.52	4.46	24
35	81	18	1	6	3.04	16.22	2.73	4.51	22
36	42	48	10	4.5	8.77	18.29	9.12	3.11	510
37	42	48	10	4.5	8.69	18.22	8.45	2.33	340
38	42	48	10	4.5	8.43	17.99	8.67	2.10	400
39	42	48	10	5	6.31	17.10	12.51	2.60	420
40	42	48	10	5	6.22	17.03	11.43	2.81	460
41	42	48	10	5	6.04	16.86	10.69	2.68	450
42	42	48	10	5.5	4.69	16.69	12.25	2.94	440
43	42	48	10	5.5	4.72	16.71	12.99	3.01	500
44	42	48	10	5.5	4.19	16.25	12.74	2.89	480
45	42	48	10	6	3.82	16.94	12.79	3.61	450
46	42	48	10	6	4.45	17.48	11.85	2.60	420
47	42	48	10	6	3.95	17.05	12.96	3.26	500
48	42	48	10	6.5	3.80	17.92	12.55	3.64	480
49	42	48	10	6.5	3.88	17.98	12.26	3.20	440
50	57	37	6	4.5	6.52	16.26	9.85	3.04	290
51	57	37	6	4.5	6.00	15.80	11.32	3.32	260
52	57	37	6	4.5	6.50	16.25	10.64	2.65	230
53	57	37	6	5	4.43	15.42	13.64	3.42	340
54	57	37	6	5	4.69	15.65	10.50	2.82	300
55	57	37	6	5.5	3.83	15.91	11.17	3.63	370
56	57	37	6	5.5	4.18	16.22	11.93	3.39	380
57	57	37	6	5.5	4.08	16.14	10.23	3.69	380
58	57	37	6	6	3.70	16.81	11.42	4.16	350
59	57	37	6	6	2.69	15.94	10.29	3.24	370
60	57	37	6	6.5	3.02	17.23	10.16	3.82	320
61	57	37	6	6.5	2.95	17.17	10.45	3.68	280
62	72	26	2	4.5	5.38	15.24	10.20	3.42	60
63	72	26	2	4.5	5.06	14.95	9.80	2.54	48
64	72	26	2	4.5	5.43	15.29	9.69	3.14	80
65	72	26	2	5	4.29	15.29	10.90	3.85	65
66	72	26	2	5	4.24	15.25	11.26	3.42	75
67	72	26	2	5	4.23	15.24	11.53	3.45	60
68	72	26	2	5.5	3.61	15.72	10.76	3.81	44
69	72	26	2	5.5	3.70	15.80	10.53	3.96	80
70	72	26	2	5.5	3.73	15.82	10.40	4.03	60
71	72	26	2	6	3.05	16.25	9.35	4.09	65
72	72	26	2	6	3.11	16.30	9.30	4.29	52
73	72	26	2	6.5	2.82	17.06	7.90	4.52	60
74	72	26	2	6.5	3.16	17.34	8.39	4.39	44
75	72	26	2	6.5	3.02	17.23	8.10	4.60	50
76	33	57	10	5	8.43	18.98	4.61	2.55	320
77	33	57	10	5	8.38	18.94	4.34	2.35	320
78	33	57	10	5	8.31	18.87	5.02	2.83	300
79	33	57	10	5.5	6.60	18.35	6.81	2.73	340
80	33	57	10	5.5	6.36	18.15	6.32	2.72	300
81	33	57	10	5.5	6.47	18.24	6.57	2.73	380
82	33	57	10	6	4.97	17.93	9.67	2.56	380
83	33	57	10	6	5.27	18.19	9.14	2.81	340
84	33	57	10	6	5.03	17.99	10.24	2.91	320
85	33	57	10	6.5	3.73	17.86	11.25	2.89	400
86	33	57	10	6.5	3.76	17.88	13.03	3.01	400
87	33	57	10	6.5	4.43	18.46	11.96	3.45	380
88	33	57	10	7	3.28	18.46	8.36	3.10	360
89	33	57	10	7	3.96	19.04	7.55	3.30	370

Table 7 (continued)

Test No.	C(%)	S(%)	F(%)	BP(%)	V _o (%)	VMA(%)	M(kN)	F(mm)	F _n
90	33	57	10	7	3.70	18.82	8.93	3.49	350
91	50.5	43.5	6	5	7.48	18.13	9.25	2.80	180
92	50.5	43.5	6	5	7.30	17.96	9.52	3.21	160
93	50.5	43.5	6	5	7.62	18.25	9.31	2.88	210
94	50.5	43.5	6	5.5	5.79	17.63	10.98	3.36	270
95	50.5	43.5	6	5.5	5.50	17.38	10.72	2.91	230
96	50.5	43.5	6	6	4.01	17.08	12.88	3.60	270
97	50.5	43.5	6	6	4.48	17.49	9.87	3.12	300
98	50.5	43.5	6	6	4.06	17.13	12.62	3.11	220
99	50.5	43.5	6	6.5	3.70	17.81	10.86	3.15	240
100	50.5	43.5	6	6.5	3.68	17.79	10.61	3.52	260
101	50.5	43.5	6	6.5	3.61	17.74	11.44	3.49	260
102	50.5	43.5	6	7	3.81	18.89	9.71	3.50	250
103	50.5	43.5	6	7	3.40	18.54	9.93	3.32	220
104	50.5	43.5	6	7	3.14	18.32	9.89	3.69	240
105	68	30	2	5	5.35	16.22	10.03	3.48	50
106	68	30	2	5	5.53	16.38	9.52	2.64	40
107	68	30	2	5	5.47	16.32	8.66	3.55	45
108	68	30	2	5.5	4.67	16.64	10.11	3.21	45
109	68	30	2	5.5	4.38	16.38	8.89	2.64	50
110	68	30	2	5.5	4.36	16.36	9.83	4.02	50
111	68	30	2	6	3.74	16.83	9.34	3.29	55
112	68	30	2	6	3.42	16.55	9.57	3.30	60
113	68	30	2	6	4.00	17.05	9.71	3.40	55
114	68	30	2	6.5	3.46	17.59	9.12	3.48	50
115	68	30	2	6.5	3.36	17.51	9.22	3.25	60
116	68	30	2	6.5	3.02	17.21	9.55	3.36	60
117	68	30	2	7	3.36	18.49	9.01	3.51	50
118	68	30	2	7	2.74	17.97	8.24	3.37	45

References

- Alavi, A. H., Ameri, M., Gandomi, A. H., & Mirzahosseini, M. R. (2010). Formulation of flow number of asphalt mixes using a hybrid computational method. *Construction and Building Materials*. doi:10.1016/j.conbuildmat.2010.09.01.
- Alavi, A. H., & Gandomi, A. H. (in press). A robust data mining approach for formulation of geotechnical engineering systems. *International Journal of Computer Aided Methods in Engineering-Engineering Computations*.
- Alavi, A. H., Gandomi, A. H., Mollahasani, A., Heshmati, A. A. R., & Rashed, A. (2010). Modeling of maximum dry density and optimum moisture content of stabilized soil using artificial neural networks. *Journal of Plant Nutrition and Soil Science*, 173(3), 368–379.
- Alavi, A. H., Gandomi, A. H., Sahab, M. G., & Gandomi, M. (2010). Multi expression programming: A new approach to formulation of soil classification. *Engineering with Computers*, 26(2), 111–118.
- ASTM, (1993). *Standard test method for resistance to plastic flow of bituminous mixtures using marshall apparatus*. ASTM D1559.
- Bahuguna, S. (2003). *Permanent deformation and rate effects in asphalt concrete: Constitutive modeling and numerical implementation*. Ph.D. Thesis. Case Western Reserve University.
- Banzhaf, W., Nordin, P., Keller, R., & Francone, F. D. (1998). Genetic programming – An introduction. *On the automatic evolution of computer programs and its application*. Heidelberg/San Francisco: dpunkt/Morgan Kaufmann.
- Baykasoğlu, A., Gullub, H., Canakci, H., & Ozbakir, L. (2008). Prediction of compressive and tensile strength of limestone via genetic programming. *Expert Systems with Applications*, 35(1–2), 111–123.
- Cevik, A. (2007). A new formulation for web crippling strength of cold-formed steel sheeting using genetic programming. *Journal of Constructional Steel Research*, 63(7), 867–883.
- Cevik, A., & Cabalar, A. F. (2009). Modelling damping ratio and shear modulus of sand-mica mixtures using genetic programming. *Expert Systems with Applications*, 36(4), 7749–7757.
- Ceylan, H., Schwartz, C. W., Kim, S., & Gopalakrishnan, K. (2009). Accuracy of predictive models for dynamic modulus of hot-mix asphalt. *Journal of Materials in Civil Engineering*, 21, 286–293.
- Chehab, G. R., Kim, Y. R., Witczak, M. W., & Bonaquist R. (2004). Prediction of thermal cracking behavior of asphalt concrete using the viscoelastoplastic continuum damage model. In *83rd annual meeting of the transportation research board*. Washington, DC.
- Chen, D. H., Zaman, M., & Laguros, J. G. (1994). Assessment of distress models for prediction of pavement service life, infrastructure: New materials and methods of repair. In *Proceedings of the 3rd materials engineering conference* (pp. 1073–1080). San Diego, CA: ASCE.
- Cybenko, J. (1989). Approximations by superpositions of a sigmoidal function. *Mathematics of Control, Signals, and Systems*, 2, 303–314.
- Eberhart, R. C., & Dobbins, R. W. (1990). *Neural network PC tools: A practical guide*. San Diego, CA: Academic Press Professional Inc.
- FHWA, (1998). *Interim task C report of preliminary recommendations for the simple performance test*. Report No. DTFH 61-94-R-00045.
- Gandomi, A. H., Alavi, A. H., Kazemi, S., & Alinia, M. M. (2009). Behavior appraisal of steel semi-rigid joints using linear genetic programming. *Journal of Constructional Steel Research*, 65(8–9), 1738–1750.
- Gandomi, A. H., Alavi, A. H., Mirzahosseini, M. R., & Moqhadas Nejad, F. (2010). Nonlinear genetic-based models for prediction of flow number of asphalt mixtures. *Journal of Materials in Civil Engineering – ASCE*. doi:10.1061/(ASCE)MT.1943-5533.0000154.
- Gandomi, A. H., Alavi, A. H., & Sadat Hosseini, S. S. (2008). A discussion on genetic programming for retrieving missing information in wave records along the west coast of India. *Applied Ocean Research*, 30(4), 338–339.
- Garson, G. D. (1991). Interpreting neural-network connection weights. *AI Expert*, 6(7), 47–51.
- Gibson, N. H. (2006). *A viscoelastoplastic continuum damage model for the compressive behavior of asphalt concrete*. Ph.D. Dissertation. College Park, MD: University of Maryland.
- Gibson, N. H., Schwartz, C. W., Schapery, R. A., & Witczak, M. W. (2003). Viscoelastic, viscoplastic, and damage modeling of asphalt concrete in unconfined compression. *Transportation Research Record*, 1860, 3–15.
- Guzelbey, I. H., Cevik, A., & Gogus, M. T. (2006). Prediction of rotation capacity of wide flange beams using neural networks. *Journal of Constructional Steel Research*, 62(10), 950–961.
- Haddadi, S., Ghorbel, E., & Laradi, N. (2008). Effects of the manufacturing process on the performances of the bituminous binders modified with EVA. *Construction and Building Materials*, 22(6), 1212–1219.
- Haykins, S. (1999). *Neural networks – A comprehensive foundation* (2nd ed.). Englewood Cliffs, NJ: Prentice Hall International Inc.
- Hinischloglu, S., & Agar, E. (2004). Use of waste high density polyethylene as bitumen modifier in asphalt concrete mix. *Materials Letters*, 58(3–4), 267–271.
- Hitch, L. S., & Russell, R. B. C. (1977). *Bituminous bases and surfacings for low-cost roads in the tropics*. TRRL Supl. Rep. Vol. 45, No. 1807. Berkshire, UK: Highways and Road Construction International.
- Hofstra, A., & Klomp, A. J. G. (1972). Permanent deformation of flexible pavements under simulated road traffic conditions. In *Proceedings of the 3rd international conference on the structural design of asphalt pavements*, London (Vol. 1, pp. 613–621).
- IAHC, (2000). *Iran Highway Asphalt Code*. No. 234. Iran: Iran Ministry of Road and Transportation, Management and Planning Organization. ISBN: 964-425-369-8.
- Johari, A., Habibagahi, G., & Ghahramani, A. (2006). Prediction of soil-water characteristic curve using genetic programming. *Journal of Geotechnical and Geoenvironmental Engineering – ASCE*, 132(5), 661–665.
- Kaloush, K. E. (2001). *Sample performance test for permanent deformation of asphalt mixtures*. Ph.D. Thesis. Arizona State University.
- Kaloush, K. E., & Witczak, M. W. (2002). Tertiary flow characteristics of asphalt mixtures. *Journal of the Association of Asphalt Paving Technologists*, 71, 278–306.

- Kannemeyer, L., & Visser, A. T. (1995). *Calibration of HDM-III performance models for use in pavement management of South African national roads*. Transportation Research Record No. 1508. Washington, DC (pp. 31–38).
- Kenis, W. J. (1977). Predictive design procedures: A design method for flexible pavements using the VESYS structural subsystem. *Proceedings of the 4th international conference on the structural design of asphalt pavements* (Vol. 1). The University of Michigan.
- Kim, Y. R. (2008). *Modeling of asphalt concrete* (1st ed.). New York: McGraw-Hill.
- King, S. (2003). *UTMS software reference manual, Version: V1:00*. UK: Wykeham Farrance International.
- Koza, J. (1992). *Genetic programming, on the programming of computers by means of natural selection*. Cambridge, MA: MIT Press.
- Kuloglu, N. (1999). Effect of astragalus on characteristics of asphalt concrete. *Journal of Materials in Civil Engineering*, 11(4), 283.
- Lavin, P. (2003). *Asphalt pavements: A practical guide to design, production and maintenance for engineers and architects*. London: Spon.
- Leahy, R. B. (1989). *Permanent deformation characteristics of asphalt concrete*. Ph.D. Dissertation. College Park, MD: University of Maryland.
- Mahboub, K., & Little, D. N. (1988). *Improved asphalt concrete design procedure*. Research Report 474-1F. Texas Transportation Institute.
- Maravall, A., & Gomez, V. (2004). EVIEWS Software, Version 5. Irvine CA: Quantitative Micro Software. LLC.
- MathWorks Inc. (2007). *MATLAB the language of technical computing, Version 7.4*. MA, USA: Natick.
- Mollahasani, A., Alavi, A. H., Gandomi, A. H., & Rashed, A. (in press). High precision neural-based modeling of soil cohesion intercept. *KSCCE Journal of Civil Engineering*.
- Monismith, C. L., Epps, J. A., & Finn, F. N. (1985). Improved asphalt mix design. *Journal of the Association of Asphalt Paving Technologists*, 54, 347–406.
- Monismith, C. L., Ogawa, N., & Freeme, C. (1975). Permanent deformation of subgrade soils due to repeated loadings. *Transportation Research Record*, (537), 1–17.
- NCHRP. (2004). *Development of the 2002 guide for the design of new and rehabilitated pavement structures: Phase II*. NCHRP 1-37A. USA: American Association of State Highway and Transportation Officials.
- Nicholls, C. (1998). *Asphalt surfacings: A guide to asphalt surfacings and treatments used for the surface course of road pavements*. London, New York: E&FN Spon.
- Nijboer, L. W. (1957). Some considerations of the 'Marshall test method for investigating bituminous masses. *Strasse und Autobahn*, 210–214.
- Oltean, M. (2004). Multi expression programming source code. Available from: <<http://www.mep.cs.ubbcluj.ro/>>.
- Oltean, M., & Dumitrescu, D. (2002). *Multi expression programming*. Technical Report, UBB-01-2002. Cluj-Napoca, Romania: Babeş-Bolyai University.
- Oltean, M., & Grossan, C. (2003a). Evolving evolutionary algorithms using multi expression programming. In W. Banzhaf et al. (Eds.), *The 7th European conference on artificial life, September 14–17, Dortmund Banzhaf. LNAI* (Vol. 2801, pp. 651–658). Springer-Verlag.
- Oltean, M., & Grossan, C. (2003b). A comparison of several linear genetic programming techniques. *Complex Systems*, 14(4), 1–29.
- Pardhan, M. M. (1995). *Permanent deformation characteristics of asphalt-aggregate mixture using varied material and modeling procedure with marshall method*. Ph.D. Thesis. Montana University.
- Pirabarooban, S., Zaman, M., & Tarefder, R. A. (2003). Evaluation of rutting potential in asphalt mixes using finite element modeling. In *Annual conference of the Transportation Association of Canada, St. John's, Newfoundland and Labrador* (pp. 1–16).
- Rumelhart, D. E., Hinton, G. E., & Williams, R. J. (1986). *Learning internal representations by error propagation. Parallel distributed processing*. Cambridge: MIT Press.
- Ryan, T. P. (1997). *Modern regression methods*. New York, NY: Wiley.
- Schapery, R. A. (1999). Nonlinear viscoelastic and viscoplastic constitutive equations with growing damage. *International Journal of Fracture*, 97, 33–66.
- Shook, J. F., Finn, F. N., Witzczak, M. W., & Monismith, C. L. (1982). Thickness design of asphalt pavements – The Asphalt Institute Method. *Proceedings of the 5th international conference on the structural design of asphalt pavements* (Vol. 1, pp. 17–44). Delft, The Netherlands: Delft University of Technology.
- Sousa, J. B., Craus, J., & Monismith, C. L. (1991). Summary report on permanent deformation in asphalt concrete. *Strategic highway research program (SHRP)*. Berkeley: National Research Council, Institute of Transportation Studies, University of California.
- Tam, W. O., Solaimanian, M., & Kennedy, T. W. (2000). *Development and use of static creep test to evaluate rut resistance of super pave mixes*. Report No. FHWA-TX-1250-4. Performed in Cooperation with the US DOT, Federal Highway Administration (FHWA) and the Texas DOT.
- Tapkin, S., Cevik, A., & Usar, Ü. (2009). Accumulated strain prediction of polypropylene modified marshall specimens in repeated creep test using artificial neural networks. *Expert Systems with Applications*, 36, 11186–11197.
- Tarefder, R. A., White, L., & Zaman, M. (2005). Neural network model for asphalt concrete permeability. *Journal of Materials in Civil Engineering*, 17(1), 19–27.
- Tayfur, S., Ozen, H., & Aksoy, A. (2007). Investigation of rutting performance of asphalt mixtures containing polymermodifiers. *Construction and Building Materials*, 21(2), 328–337.
- Timm, D. H., & Newcomb, D. E. (2003). *Calibration of flexible pavement performance equations for minnesota road research project*. Transportation Research Record No. 1853. Washington, DC: National Research Council.
- Tom, V. M., & Krishna Rao, K. V. (2007). *Introduction to transportation engineering. Marshall mix design, national programme on technology enhanced learning (NPTEL)*. India: Indian Institute of Technology.
- Topal, A., & Sengoz, B. (2005). Determination of fine aggregate angularities in relation with the resistance to rutting of hot mix asphalt. *Construction and Building Materials*, 19(2), 155–163.
- Williams, C., Robinette, C. J., Bausano, J., & Breakah, T. (2007). *Testing of wisconsin asphalt mixtures for the forthcoming aashto mechanistic-empirical pavement design procedure*. Final Report. Wisconsin Highway Research Program #0092-04-07. Madison: University of Wisconsin.
- Witzczak, M. W., Kaloush, K., Pellinen, T., El-Basyouny, M., & Von Quintus, H. (2002). *Simple performance test for superpave mix design*. NCHRP Report 465. Washington, DC: National Research Council, Transportation Research Board.
- Xiao, F., Amirhanian, S., & Hsein Juang, C. (2009). Prediction of fatigue life of rubberized asphalt concrete mixtures containing reclaimed asphalt pavement using artificial neural networks. *Journal of Materials in Civil Engineering*, 21(6), 253–261.
- Zhou, F., Scullion, T., & Sun, L. (2004). Verification and modeling of three-stage permanent deformation behavior of asphalt mixes. *Journal of Transportation Engineering – ASCE*, 130(4), 486–494.
- Zoorob, S. E., & Suparna, L. B. (2000). Laboratory design and investigation of the properties of continuously graded asphaltic concrete containing recycled plastics aggregate replacement (Plastiphalt). *Cement and Concrete Composite*, 22, 233–242.